UNCLASSIFIED

Design Specifications: Simulation of Surface Surveillance System-of-Systems Success ('S6')

D.W. Mason
Directorate of Air Staff Operational Research

DRDC CORA TR 2006–05
April 2006

Defence R&D Canada
Centre for Operational Research & Analysis

Directorate of Air Staff Operational Research
Chief of the Air Staff

National Defence Défense nationale

UNCLASSIFIED

Canada

Design Specifications: Simulation of Surface Surveillance System-of-Systems Success ('S6')

D.W. Mason
Directorate of Air Staff Operational Research

DRDC – Centre for Operational Research and Analysis

Technical Report

DRDC CORA TR 2006-05

April 2006

Author

D.W. Mason

Approved by

J.R. Evans
Director of Operational Research (Maritime, Land and Air)

Approved for release by

M.T. Rey
Director General, DRDC Centre for Operational Research & Analysis

Abstract

Nations wish to have full knowledge of surface ship traffic off their coastlines, but no single surveillance asset has the presence, scope, and fidelity to perform this function completely by itself. The ideal solution will be a 'system of systems' that relies on different surveillance systems with diverse spatial, temporal, and information content characteristics working together to deliver a clear Recognized Maritime Picture (RMP). Examples of specific systems that might contribute are aircraft patrols, ship patrols, unmanned aerial vehicles, radio direction finding systems, surveillance satellites, ground-based radars, surface wave radars, or automatic identification systems (AIS).

Determination of the ideal system-of-systems requires an analytical capability to assess the effectiveness of specific combinations of systems. The preferred method for satisfying this requirement is through the development of a simulation of surface traffic, the performance of various surveillance assets operating on that traffic, and the integration of the sensor information into a RMP over time. This will be realized as the Simulation of Surface Surveillance System-of-Systems Success, or the 'S6' model, which will be developed under contract to the specifications outlined in this document.

The S6 Model will be an event-based simulation of surface ship traffic and sensor activity over an area of operations, typically one of Canada's ocean approaches. Rogue vessel tracks will be injected into the background surface traffic and the simulation will be able to assess how well the combined system-of-systems responded in acquiring and tracking these rogue vessels. There are Monte-Carlo aspects to the simulation, specifically in the generation of ship traffic and errors introduced by each sensor system in acquiring targets.

Résumé

Tout État cherche à être au courant de toute circulation maritime de navires de surface dans ses zones littorales, mais jusqu'à maintenant, aucun dispositif de surveillance n'a la présence, la portée et la fidélité nécessaires pour s'acquitter seul de cette fonction. La solution idéale repose sur un « système de systèmes » qui dépend de différents systèmes de surveillance ayant les caractéristiques spatiales, temporelles et le contenu nécessaire pour travailler de concert à dresser un tableau de la situation maritime (TSM). Parmi les systèmes particuliers qui pourraient contribuer se trouvent des avions de patrouille, des navires de patrouille, des véhicules aériens télépilotés, des systèmes radiogoniométriques, des satellites de surveillance, des radars au sol, des radars haute fréquence à ondes de surface et des systèmes d'identification automatique (SIA).

L'élaboration d'un système de systèmes idéal requiert une bonne capacité d'analyse afin d'évaluer l'efficacité de combinaisons particulières de systèmes. La méthode de prédilection en vue de satisfaire cette exigence est la mise en place d'une simulation de circulation de surface, l'utilisation de divers dispositifs de surveillance autour de cette circulation et l'intégration dans un TSM des renseignements provenant de capteurs. Cette démarche verra le jour à l'aide du Succès de la simulation d'un système de systèmes de

surveillance de surface, appelé le modèle « S6 », qui sera élaboré dans le cadre d'un contrat et selon les spécifications présentées dans ce document.

Le modèle S6 est une simulation fondée sur la réalité de la circulation maritime de navires de surface et de l'activité des capteurs dans un secteur d'opérations, généralement une des approches océaniques du Canada. Les sillages des navires suspects seront intégrés à l'arrière plan de la circulation de surface et la simulation pourra évaluer dans quelles mesures le système de systèmes combinés a réussi à acquérir et à localiser ces vaisseaux suspects. La simulation de la circulation maritime et les erreurs introduites par chaque système de capteurs dans l'acquisition d'objectifs sont des effets Monte-Carlo possibles.

EXECUTIVE SUMMARY

In today's world of global terrorism it is more critical than ever for Canada to have full knowledge of the surface ship traffic off its coastlines. No single surveillance asset has the presence, scope, and fidelity to perform this function completely by itself. The ideal solution will be a 'system of systems' that relies on different surveillance systems with diverse spatial, temporal, and information content characteristics working together to deliver a clear Recognized Maritime Picture (RMP).

One way of investigating possible solutions is through the development of a simulation of the target/sensor environment over space and time. It would be useful to have a simulation that represents the surface traffic, the performance of various surveillance assets operating on that traffic, and the integration of this surveillance information into a RMP over time. This vision will be realized as the Simulation of Surface Surveillance System-of-Systems Success, or the 'S6 Model', which will be developed under contract to the specifications outlined in this document.

The S6 Model will simulate the activity of surface traffic and surveillance sensors and platforms over an area of operations – typically one of Canada's ocean approaches. The Graphical User Interface (GUI) will be built around a map-like presentation, which may be built on Geographic Information System (GIS) products.

The S6 Model will be an event-sequenced, Monte-Carlo simulation. Some events will inject new surface traffic targets into the region at random times, and others will simulate the production of sensor information overlays as the various components of the system of systems perform, with random errors introduced (including the ability to miss targets or generate false targets).

Nine general classes of sensors will be represented: aircraft patrols (both pre-planned and reactive); ship patrols; unmanned aerial vehicles; passive direction finding systems (high frequency radio or acoustic); surveillance satellites; ground-based radars; surface wave radars; and self-reporting schemes including automatic identification systems (AIS). The challenge has been to represent the performance of these sensor classes as directly as possible. Simple, 'cookie-cutter' representations have been designed in all cases, and are described in detail in this report.

One of the key modelling constructs is the handling of positional uncertainty about a target in the RMP, and its growth over time in the absence of updated information. The construct used is based on the Circular Normal distribution.

Data fusion must be a central process within any model of this type. Since the purpose is to compare various systems of systems in overall effectiveness, it is important to model the data fusion process, not necessarily like it should be done ideally, but rather like it would be done in real life. Therefore, the S6 Model will have 'roughed in plumbing' for the inclusion of any desired data fusion algorithm that accepts the current RMP and an overlay of sensor information from a single source, and then calculates an updated RMP. A simple, forced-matching type of algorithm is presented in this report to serve as a default choice for the user.

Information latency is an important property to consider while developing and maintaining a RMP, and it is a challenge to model. Surveillance information that arrives after some delay may not be a problem if the data fusion system can back up its process to the point in time when the information was fresh, integrate that information, and then re-integrate the information that arrived after that point in time. But if the fusion process has no time rollback ability, late information may quickly become useless. The S6 Model will permit users to establish where between these two end points on this spectrum they would like to operate.

It is important to employ the right measures of effectiveness (MOEs) in any analysis. Effectiveness within the S6 Model is measured by performance of the combined system of systems against rogue targets injected by the user into the traffic stream. The ability of the system to detect, classify, or identify these targets before they reach critical waypoints in their paths is measured.

The Defence Research and Development Canada (DRDC) Centre for Operational Research & Analysis (CORA) and the Chief of the Air Staff (CAS) will jointly fund the contracted development of the S6 Model to the design specifications in this document. When completed, this analysis tool will support decisions, not only on potential aerospace solutions to the coastal surveillance problem, but on the full spectrum of possible solutions that would comprise a robust 'system of systems'.

SOMMAIRE

Dans le monde d'aujourd'hui sous la menace constante du terrorisme, il est encore plus important pour le Canada d'avoir une connaissance réelle de la circulation maritime de navires de surface dans ses zones littorales. Aucun dispositif unique de surveillance n'a la présence, la portée et la fidélité nécessaires pour s'acquitter seul de cette fonction. La solution idéale repose sur un « système de systèmes » qui dépend de différents systèmes de surveillance ayant les caractéristiques spatiales, temporelles et le contenu nécessaire pour travailler de concert à dresser un Tableau de la situation maritime (TSM) clair.

L'élaboration d'une simulation de l'environnement cible et de capteurs dans l'espace et dans le temps permet de déterminer des solutions possibles. Il serait utile d'avoir une simulation qui représente la circulation maritime de surface, le rendement de divers dispositifs de surveillance traitant de cette circulation et l'intégration de ces renseignements de surveillance dans un TSM à un moment donné. Cette démarche verra la jouer par le Succès de la simulation d'un système de systèmes de surveillance de surface, appelé le « modèle S6 », qui sera élaboré dans le cadre d'un contrat et selon les spécifications précisées dans ce document.

Le modèle S6 simulera les activités des capteurs et des plates-formes de circulation de surface et de surveillance dans un secteur d'opérations, généralement une des approches océaniques du Canada. L'interface graphique (GUI) sera élaborée autour d'une présentation analogue à une carte pouvant être élaborée à l'aide de produits de système d'information géographique (SIG).

Le modèle S6 est une simulation Monte-Carlo, un programmateur séquentiel d'événements. Certaines activités ajouteront de nouveaux objectifs de circulation maritime de surface de manière aléatoire dans une région et d'autres activités simuleront la production de segments de recouvrement d'information de capteurs au fur et à mesure que les différents composants du système des systèmes exécutent leurs tâches et que des erreurs sont introduites de manière aléatoire (y compris la capacité de manquer les objectifs et de générer de faux objectifs).

Neuf catégories générales de capteurs seront représentées : les patrouilles aériennes (prévues et répressives), les patrouilles de navire, les véhicules aériens télépilotés, les systèmes radiogoniométriques passifs (radio à haute fréquence et acoustique), les satellites de surveillance, les radars au sol, les radars haute fréquence à ondes de surface et les méthodes d'autovérification, y compris les systèmes d'identification automatique (SIA). Le problème repose sur la représentation du rendement de ces catégories de capteurs aussi directement que possible. Des représentations simples et en série ont été conçues pour tous les cas et elles sont décrites en détail dans ce rapport.

L'une des principales modélisations conçues touchent la considération de l'incertitude dans le positionnement de la cible dans le TSM et l'accroissement de cette incertitude dans le temps en l'absence de données actualisées. Le modèle utilisé est fondé sur la courbe en cloche normale.

La fusion de données doit constituer un processus central dans un modèle de ce type. Comme l'objectif est de comparer différents systèmes de systèmes dans leur efficacité globale, il importe de modeler le processus de fusion des données comme cela serait fait dans la réalité plutôt que de la manière idéale. Ainsi, le modèle S6 disposera des fondements nécessaires à l'inclusion de tout algorithme de fusion de données souhaitées qui accepte le TSM actuel et la superposition de renseignements de capteurs provenant d'une seule source et fera ensuite les calculs nécessaires pour arriver à un TSM actualisé. Un type d'algorithme simple d'appariement forcé est également présenté dans ce rapport et sera l'option par défaut pour l'utilisateur.

Les renseignements secrets constituent une propriété importante à prendre en considération dans l'élaboration et le maintien du TSM et un défi de taille pour la modélisation. Les renseignements de surveillance qui arrivent avec un certain délai ne représentent pas nécessairement un problème si le système de fusion des données peut revenir en arrière dans son processus jusqu'au moment où les renseignements étaient actuels, les intégrer et ensuite réintégrer les renseignements qui sont arrivés plus tard. Mais si le processus de fusion n'a aucune capacité de retour en arrière, les renseignements tardifs deviennent rapidement inutiles. Le modèle S6 permettra aux utilisateurs de déterminer où ils aimeraient établir les opérations entre les deux paramètres ultimes du spectre.

Il importe d'utiliser les mesures d'efficacité (ME) adéquates dans une analyse. L'efficacité du modèle S6 est évaluée par le rendement du système de systèmes combinés par rapport aux objectifs suspects ajoutés par l'utilisateur dans le flot de circulation. On évaluera également la capacité du système d'identifier, de classifier et de relever ces objectifs avant qu'ils n'atteignent le point de cheminement de leur trajectoire.

Le Centre de recherche opérationnelle et d'analyse (CROA) de Recherche et développement pour la Défense Canada (RDDC) et le Chef d'état-major de la Force aérienne (CEMFA) financeront conjointement le contrat d'élaboration du modèle S6, selon les spécifications précisées dans ce document. Lorsqu'il sera complété, cet outil d'analyse permettra d'appuyer les décisions non seulement en ce qui concerne les solution aérospatiales possibles au problème de surveillance du littoral, mais également toute la gamme de solutions possibles qui comprendraient un « système de systèmes » rigoureux.

Table of Abbreviations

AIS	Automatic Identification System
CAS	Chief of the Air Staff
CEP	Circular Error Probable
CORA	Centre for Operational Research & Analysis
DASOR	Directorate of Air Staff Operational Research
DF	Direction Finding
DRDC	Defence Research & Development Canada agency
GIS	Geographic Information System
GOV	Government vessel patrol (sensor type)
GUI	Graphical User Interface
HCF	Heading Consistency Factor
HFDF	High Frequency Direction Finding
ILF	Information Latency Factor
MARLANT	Maritime Forces Atlantic
MARPAC	Maritime Forces Pacific
MOE	Measure of Effectiveness
MTBF	Mean Time Between Failures
MTTR	Mean Time To Repair
OR	Operational Research
P-AIR	Pre-planned Aircraft patrol (sensor type)
RAD	Radar, ground-based (sensor type)
R-AIR	Reactive Aircraft patrol (sensor type)
RAPDC	Reactive Air Patrol Demand Check (event type)
RMP	Recognized Maritime Picture

RPU	Radius of Positional Uncertainty
RV	Regional View
S6	Simulation of Surface Surveillance System-of-System Success
SAR	Synthetic Aperture Radar
SAT	Satellite (sensor type)
SD	Sensor Data (information generator)
SRP	Self-Reporting Policy
SRS `	Self-Reporting System
SS	Surface Ship (target generator)
SWR	Surface Wave Radar
TR	Trigger Regions (for RAPDC event)
TT	Tracked Target (in the RMP)
UAV	Unmanned Aerial Vehicle

Table of Contents

1. INTRODUCTION

1.1 Background

1. In today's world of global terrorism it is even more critical for Canada to have full knowledge of the surface traffic off its coastlines. This problem of determining the quality and quantity of surveillance required to deliver this knowledge has been a ongoing focus of Operational Research (OR) efforts over the years.

2. In reviewing recent OR studies on coastal surveillance, and relying on Fisher [1] who reviewed studies prior to 1991, the following broad summary of previous efforts in this field is offered. The application of fundamental search theory in developing abstract area and barrier patrol tactics is a classical OR field that has been well addressed by past studies. The contributions of individual new sensors and platforms, such as a new aircraft fleet, Synthetic Aperture Radar (SAR) onboard a satellite, or Surface Wave Radar (SWR), or the impact of a change in the political landscape (200 mile limit) or emerging threats (migrant smugglers) have been regularly investigated as well. The effectiveness of multiple sensor types working together to deliver a collective surveillance capability has been tackled previously (for example, Mason [2]). Typically, such studies have employed measures of effectiveness (MOE) such as the mean revisit times. Recently, Fong [3] incorporated multiple sensors within the context of a physics-based simulation environment (SIMLAB), using the ability to synthesize the individually produced target tracks as the combined effectiveness indicator. Both Dickinson et al [4] and Bourdon et al [5] discussed the challenges of developing MOEs in this domain, and identified measures at the highest levels (force effectiveness measures), including scenario-based effectiveness measures that key on the interdiction of specific threat vessels.

3. It is acknowledged that no single surface surveillance asset has the presence, scope, and fidelity to perform the coastal surveillance function completely by itself. The ideal solution will be a 'system of systems' that relies on different surveillance systems with diverse spatial, temporal, and information content characteristics working together to deliver a clear Recognized Maritime Picture (RMP). Examples of specific systems that might contribute are aircraft patrols, ship patrols, unmanned aerial vehicles, radio direction finding systems, surveillance satellites, ground-based radars, surface wave radars, or automatic identification systems (AIS).

4. Determination of the ideal system-of-systems requires an analytical capability to assess the effectiveness of specific combinations of systems. The preferred method for satisfying this requirement is through the development of a model that simulates the surface traffic, the performance of various surveillance assets operating on that traffic, and the integration of the sensor information into a RMP over time. Scenario-based MOEs would be extracted, keying on combined capability against various threat targets injected into the surface traffic. This will be realized as the Simulation of Surface Surveillance System-of-Systems Success, or the 'S6' model, which will be developed under contract to the specifications outlined in this document.

5. The Defence Research and Development Canada Centre for Operational Research & Analysis (DRDC CORA) and the Chief of the Air Staff (CAS) will jointly fund the contracted development of the S6 Model to the design specifications in this document.

When completed, this analysis tool will support decisions, not only on potential aerospace solutions to the coastal surveillance problem, but on the full spectrum of possible solutions that would comprise the best 'system of systems'.

1.2 S6 Model General Description

6. The S6 Model will simulate background surface vessel traffic over an area of operations – typically one of Canada's ocean approaches. In an event-sequenced fashion, the simulation will generate the targeting outputs from the various sensor systems within the system-of-systems. Going through a data fusion process, it will then rectify the new surveillance information layer with the current RMP to generate an updated RMP.

7. Rogue vessel tracks will be injected into the background surface traffic and the simulation will be able to assess how well the system-of-systems responded in acquiring these rogue vessels.

8. There are Monte-Carlo aspects to the simulation, specifically in the generation of ship traffic, errors introduced by each sensor system in acquiring targets, and the timing of rogue vessel tracks.

9. The simulation will simulate a user-specified period of time and will generate a summary of the results.

10. One of the major design decisions when constructing a simulation of the performance of physical systems, such as sensors, is the level of detail to which those systems are modelled. There are generally two options – a detailed, low level, physics-based approach, or a simpler, high-level, probability based approach. For the S6 model the latter choice was made. The purpose of the model will be to investigate sensor system tradeoffs at a very high level, so there is little added value in simulating the one-on-one performance of candidate systems in intensive detail. Simple models that capture the performance dependencies of each sensor permit the model to focus on overall performance. Of course, physics-based performance models may be required to generate the inputs to the simpler model, especially for conceptual or untested systems.

2. S6 MODEL REPRESENTATIONS

11. The major modelling concepts and constructs for the proposed S6 model are described in this section. Requirements for the Graphical User Interface (GUI) will be outlined as the descriptions unfold.

2.1 Representation of Time

12. The spine of the S6 simulation model will be the event manager. Simulated time will advance to the time of the next event in the queue. These events will be: to inject a new surface ship target into the traffic; to simulate the information overlay produced by a sensor; to perform the fusion of the sensor data with the RMP; or to assess the current RMP and determine whether reactive sensor resources (e.g. aircraft patrols) should be scheduled.

13. Each Sensor Data (SD) information overlay generation event will use global routines to determine the 'ground truth' positions of all Surface Ship (SS) traffic at a point in time, and then will simulate the production of a SD overlay rendered on that traffic. The event will simulate the generation of knowledge on targets in the traffic, gathering a (possibly incomplete) list of information on target classification or identity, position, and velocity vector (speed and heading). Sensor performance will be based not only on fundamental parameters such as range to the target, but will also represent various types of target acquisition errors in a Monte Carlo fashion, including missed and false targets. Each event will then schedule its next occurrence in time.

14. Chapter 4 provides detailed descriptions of how each type of sensor is to be modelled, including a list of the input parameters and algorithmic foundation for that sensor type. Nine different classes of sensors are presented.

15. Every Sensor Data event will automatically trigger a Data Fusion (DF) event on its completion, passing on the targeting information collected in this SD overlay, along with quantifications of the error associated with the position, speed, and heading estimates rendered. The RMP at that time will consist of a number of Tracked Targets (TT) with an identical set of (again, possibly incomplete) attributes. Simply stated, the Data Fusion event merges the old RMP and the new SD overlay using a set of rules to produce an updated RMP.

16. Several data fusion algorithms can be available, each with its own separate code written, with the user selecting which one is to be applied during the current run. The initial implementation of the S6 model will contain a single, simple, data fusion algorithm as the default choice. This algorithm is described in detail in Chapter 5.

17. Finally, a Reactive Air Patrol Demand Check, or 'RAPDC' event, will be executed to determine whether the updated RMP contains a TT that has yet to be identified and is within a region of concern. If so (and if a monthly limit on the number of reactive air patrols has not been exceeded) then a Reactive Air Patrol (see R-AIR event description) will be scheduled.

18. Execution will terminate at a user specified simulation time limit, at which time the user-selected Measures of Effectiveness (MOE) will be presented. Chapter 6 presents a discussion of the MOEs and how they are to be collected and delivered.

19. The simulation time clock begins at 0 hours, which will be midnight on the first day of simulated time in the time zone of the origin of the region being viewed. It is required to track time of day (i.e. time modulo 24 hrs) in order to model sun-synchronous satellites and systems with diurnal variability in performance such as surface wave radar. On some occasions, like the RAPDC event above, it is also required to track the month.

20. Seasonal variability is assumed to be beyond the anticipated time scale of any particular run. Certainly, traffic patterns can vary seasonally, and selected sensors may perform differently by season. These variations are assumed to be represented within the parameter set established for any given run scenario.

2.2 Representation of Space

21. The primary graphical display will be a map-like presentation showing land and water features, overlaid with the three key layers of information:

a. The underlying ‘ground truth’ of all SS traffic;

b. The set of TT comprising the current RMP; and

c. Any new SD overlay generated.

22. The underlying screen map will necessarily be a Cartesian, ‘flat-earth’ projection. Although the core of the simulation and its underlying algorithms will operate in the Cartesian coordinate system whenever possible, some events - such as a satellite pass generating sensor data - will clearly have to operate in the spherical coordinate domain initially. This makes it essential to be able to convert when required from spherical to Cartesian coordinates.

23. The orthographic map projection, which provides a view of the earth from infinity above a selected ‘zenith’ point on the surface of the earth, is one reasonable choice to implement. A discussion of map projections and an outline of the mathematics of orthographic projections are presented in Annex A (see also Lindsey [6]). The contractor has the option of utilizing any reasonable map projection scheme, but must provide the algorithmic foundation for accurate conversion from spherical (i.e. latitude and longitude) to Cartesian (i.e. flat earth) coordinates.

24. A Regional View (RV) will define the entire Cartesian ‘playing field’ for the simulation run. The origin of this coordinate system will represent a *central latitude* and *longitude* on the earth, and the dimensions of the playing field will be defined by maximum x and y values, in nautical miles. If X_{Max} and Y_{Max} represent these limits, then the RV is the region bounded by $(\pm X_{Max}, \pm Y_{Max})$. The proportions of the RV area may or may not match the proportions of the map display window, but the user will be able to zoom and pan around the entire RV at any time during the setup and execution phases of the simulation run.

25. The contractor will provide at least two initial Regional Views – representing Canada's east and west coasts and their approaches. The simulation will include the ability for the user to establish new RVs where desired geographically. The user will select the RV to be used for the current run.

26. The contractor is free to propose the basic map display format – a raster map image or a vector drawn image. In selecting the format, consideration should be given to the ability to easily generate new RVs around the globe, as needed. The acquisition of Geographic Information System (GIS) products is an anticipated requirement.

27. Besides providing the ability to efficiently zoom and pan the RV, the GUI will also echo the position of the cursor (within the Cartesian coordinate system) in a visible text box.

28. Each Ship Class will have a small icon with a distinctive shape associated with it (see Chapter 3 for a discussion of all Ship Class attributes). Each icon will have a definitive orientation that will be used to depict the current heading of the particular instance of that class being displayed. If a raster graphics presentation of the icons is employed, the orientation displayed must be within ±5 degrees of its true heading. The contractor will design at least 15 different icons to assign to the various ship classes. They should be composed of shades of a single colour, mixed optionally with shades of grey, and might look something like the following simplistic shapes:

Δ □ □ □ □ □ □ □ □ □ □

29. Ship Class icons will be displayable in different colours (substituting for the single colour in the icon), depending on the information layer and/or the level of target acquisition being displayed.

30. We will use the unique maritime term 'datum', the singular of 'data', to refer to the set of information on a single acquired target in the SD overlay.

31. For each detection 'datum' in the SD overlay, or for each TT in the RMP that has not yet been classified or identified, a simple, circular, 'detection only' icon will be associated with its location. If the sensor was able to produce a velocity vector estimate for that datum, or if the TT has a velocity vector determined, then that heading must be able to be displayed as well to within an accuracy of ±5 degrees of its value. The following are possible examples of the 'detection only' and 'detection only with heading' icons:

○ ● □ □ ♂ ô

32. It may happen that a SD or TT are classified or identified but no velocity vector has been established. In this case the icon would have a default orientation (pointing due north perhaps).

33. The above structure is suggestive only. Considerable leeway is given to the contractor to design the map and information overlay presentations. It will be important to use the colour dimension effectively in designing a clear presentation of the various overlays to the user.

34. The user will be able to select the overall level of display of simulation activity and change it as the simulation executes:

a. No map display at all while simulation is running; simulation simply stores results and notifies user when run is complete;

b. Full display of all information layers (user selects combination) as simulated time progresses;

c. Full display that pauses after each Data Fusion event associated with a selected subset of the Sensors;

d. Full display pauses execution after Data Fusion events for all Sensors

35. The user will be able to independently and interactively toggle on or off all three layers of information. Any time a layer is activated its display is brought to the foreground. When the simulation is paused during display modes c. and d., a fourth layer is also available: the new (i.e. updated) RMP.

36. Having the full flexibility to select the desired level of display and display the four layers of information as desired is essential for quick debugging of both the code and the scenario inputs. Figure 1, presented at the end of this Chapter, provides a notional illustration of what these GUI displays might entail.

2.3 Representation of Positional Uncertainty

37. One of the central modelling constructs within the S6 simulation is the mechanism used to represent positional uncertainty of targets on the surface.

38. A general Bivariate Normal distribution is commonly employed to describe positional accuracy in two dimensions probabilistically. It suits passive cross-fixing systems such as High Frequency Direction Finding (HFDF) or passive sonar. Generally three parameters are required to define this distribution about a given position: the orientation of the major axis and the standard deviations in both the major and minor axes.

39. However, the simplified version of the Bivariate Normal, the Circular Normal, is an attractive choice of probability distribution for modelling. It requires only a single parameter to define it about a given position - the standard deviation, σ, in either orthogonal direction - and is much easier to work with. The Circular Normal is assumed to be a reasonable distribution for target location errors associated with most sensors that would operate from land, sea, air, or space. This is acknowledged to be perhaps a poorer assumption for the passive cross-fixing sensor systems mentioned above, but is adopted for practical reasons.

40. Given the Circular Normal parameter σ, the radius corresponding to a given cumulative Circular Normal probability level, Q, can be calculated. This is the radius that has a probability Q of including the actual target. The straightforward conversion

formula and a discussion of the associated Rayleigh distribution is presented in Annex C (annex content is largely derived from Emond [7]). This distance is labelled the *Radius of Positional Uncertainty* at that cumulative probability level, or RPU_Q. Sensor location errors are commonly specified as a *Circular Error Probable*, or *CEP*. This is the radius within which there is a 50% chance of locating the target. Hence, *CEP* equates to $RPU_{0.50}$.

41. One of the other key parameters within the S6 simulation is the *Positional Confidence Level,* designated simply as *P*. This is a global, user-specified parameter within the simulation that describes the nominal level of accuracy at which the RMP is to track any target. The default Data Fusion algorithm (see relevant section) and the graphical interface will employ and display concentric circles of radius RPU_P and $RPU_{\sqrt{P}}$. Typically, one would expect to use a value of *P* in the neighbourhood of 0.99, but the user can investigate the fusion algorithm behaviour at various levels of *P* to determine a most appropriate value for the analysis being conducted.

2.4 Scenarios

42. The term ‘Scenario’ is used to describe the full set of information to be executed. This includes the specification of global parameters, identification of the Regional View employed, identification of Data Fusion algorithm to be used (see Chapter 5), the full set Surface Ship traffic generators (see Chapter 3) and Sensor Data generators (see Chapter 4) to be used, and the SS target list on which the Measures of Effectiveness are to be captured (see Chapter 6). Scenarios can be saved and labelled for future use. Some of the individual traffic and sensor generators can also be saved and labelled for future use (with the same RV).

43. Finally, Figure 1 is presented as a partial, simplified, notional vision of what the screen map display might look like as a Scenario unfolds. It is provided simply to help convey some of the modelling features outlined above and should be considered illustrative, not prescriptive. The contractor is given full flexibility to apply their expertise and ingenuity in designing the appropriate GUI.

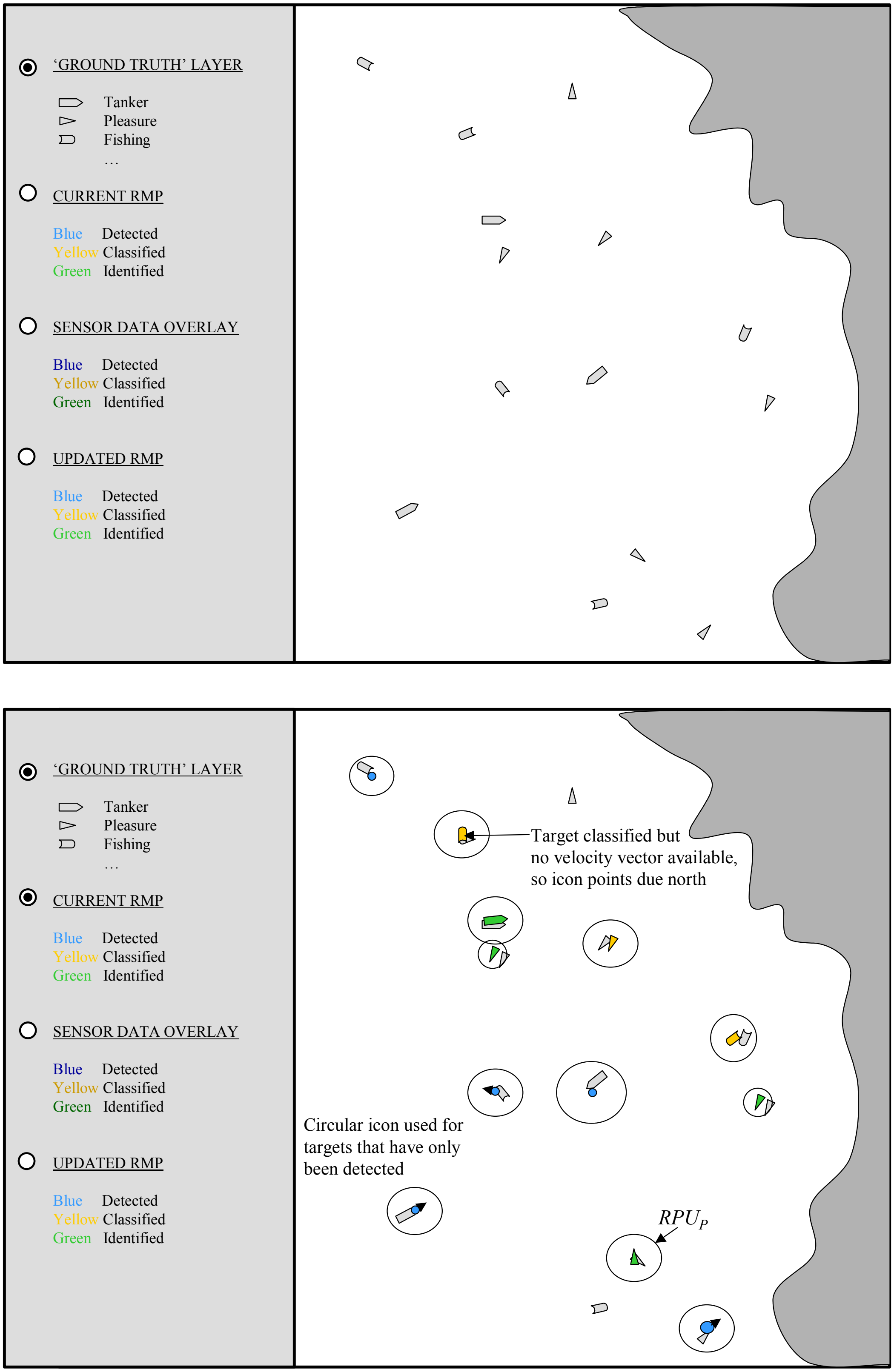

***Figure 1.** Notional Map Display Graphics*

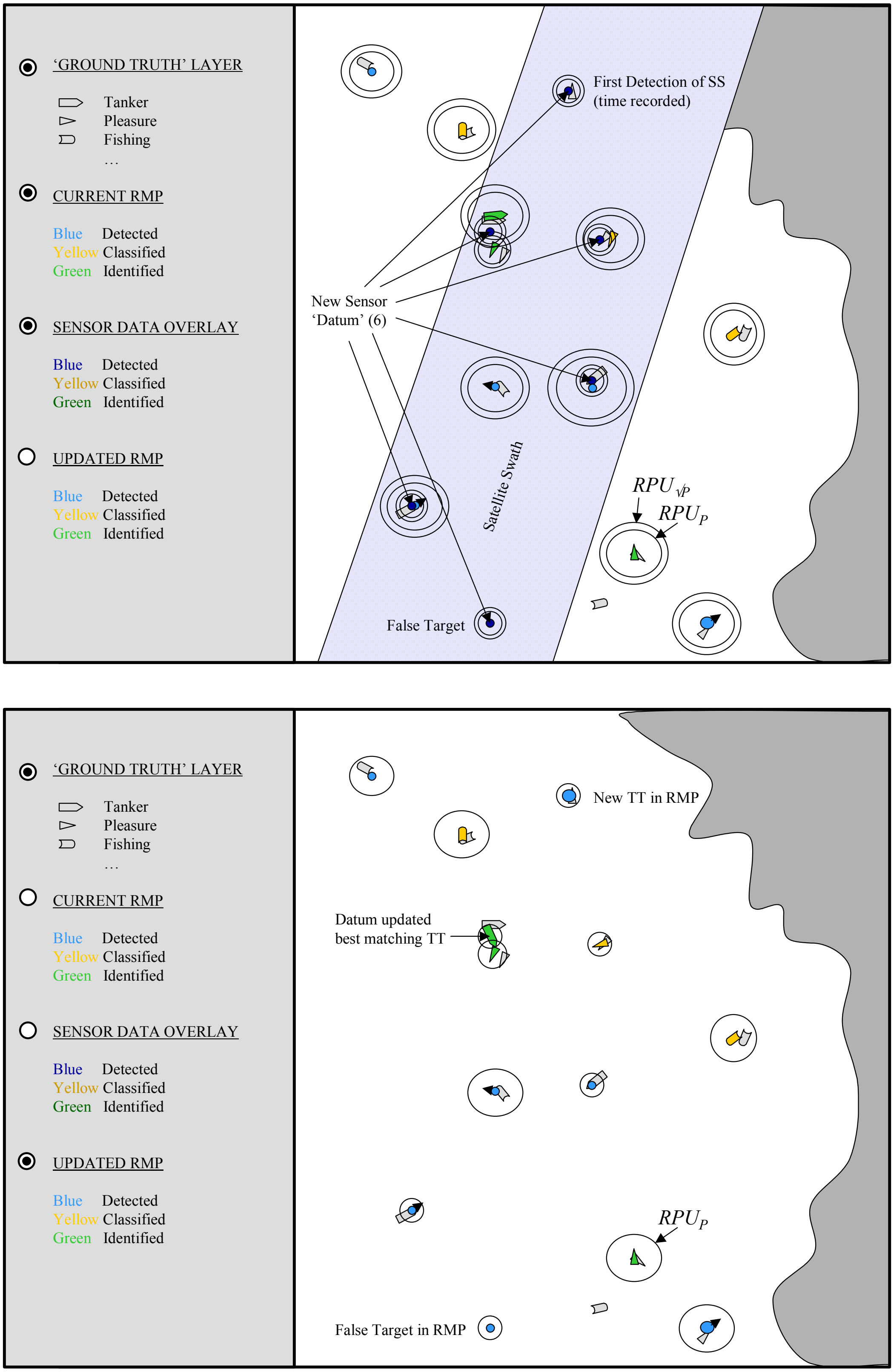

Figure 1 (cont'd). *Notional Map Display Graphics*

This page intentionally left blank.

3. SURFACE SHIP TRAFFIC GENERATORS

44. The user will re-use or create a number of surface ship traffic generators, or 'SS Generators', to feed the simulation. Each SS Generator will initiate tracks of a given Ship Class randomly over time.

45. Before describing the attributes of the SS Generator, the attributes of each **Ship Class** will be introduced. Each Ship Class has the following attributes:

a. **Class name** - alphanumeric title (e.g. "fishing boat", "supertanker", "container ship", "yacht", …)

b. **Class icon -** for map display purposes, as described in Section 2.2. Note that the icon must be able to be oriented within an accuracy of ±5 degrees when displayed with a known heading.

c. **Class maximum sustained speed** at the *P* probability level - that is, the probability is *P* that a vessel of this class would be maintaining this speed or less over an extended time. This parameter is used to estimate the distance the vessel could have possibly travelled since its last known location (see Annexes C and D).

d. **Heading Consistency Factor (HCF) -** a number between 0 and 1 that indicates whether vessels in this class are very likely (value near 1) or unlikely (value near 0) to continue following an observed heading. Annexes C and D describe how this parameter is employed. It enables the simulation to be predictive to a degree about future behaviour of target vessels (analogous to how a Kalman Filter might behave).

e. **Effective ship height** - in feet above sea level. This is used by conventional radar systems in determining their horizon against this class of ship. It is assumed that the ship's own radar would be at this height as well (see h. below).

f. **Probability ships in this class will adopt a self-reporting policy (SRP).** A random number is drawn against this probability when each SS is instantiated to determine if it is going to be a self-reporter of its position, identity, and velocity vector or not. Note that this is distinct from carrying an Automatic Identification System (AIS) transponder (see details in Chapter 4).

g. **Probability of adhering to SRP at any given update.** Despite having adopted a SRP, individual SS in this class may not always adhere to it. Reasons can be technical or procedural (e.g. they forgot). Updates are assumed independent, so lack of adherence does not persist.

h. **Class provides surveillance?** – 'Yes' or 'No'. Surveillance vessels are set up as normal ship traffic, but they will actually survey the region to the radar horizon limit off their path and provide inputs to the RMP.

They would normally be government (Coast Guard or Navy) vessels, but might be helpful commercial vessels as well. See description of the SD Generator of the GOV class in Section 4.7.

46. A **SS Generator** has the following parameters defined for it:

a. **Ship Class** – Name of the Class being generated. Note that there can be multiple SS Generators for any given Ship Class.

b. **Generator name** – e.g. ‘Container 1’, ‘Rogue 3’

c. **Generation rate** – given as an average number of new SS injected per unit time (hour). The new SS will be instantiated as part of a Poisson Process, with the generation event calculating the interval until the next generation event. Annex F describes how to randomize the first and all subsequent SS injection events.

d. **Set of Waypoint Zones -** used to define the start, end, and waypoints for any actual path generated. A zone can be a line or a convex polygon. Actual waypoints will be randomly selected within the defined zone (see selection algorithms in Annex G).

e. **Leg speed range -** maximum and minimum specified for each leg, in knots. A random speed value will be drawn uniformly between these limits and applied to the path leg.

f. **Performance against monitored?** – ‘Yes’ or ‘No’. Indicates whether vessels instantiated by this SS Generator are to be tracked for performance of the system-of-systems against them. Chapter 6 describes the Measures of Effectiveness employed for the S6 model, which include determining the acquisition status when SS reach each waypoint in their paths.

g. **Surveillance vessel parameters.** The following parameters define the capability of the surface vessel to locate and estimate the velocity vector for other SS acquired within its radar horizon. Identification of all targets is assumed, so the generation of false targets does not apply. Surveillance vessels without helicopters can be assumed to deviate off their generated path in order to identify targets, but ‘officially’ they stay on the generated path (user may enter artificially slow leg speeds to accommodate this feature if ship has no helicopter onboard)

   i. **Update interval.** Time (in hours) between surveillance updates provided to the Data Fusion algorithm

   ii. **Probability of missing a target.** The ship may miss some targets within its radar horizon every update period.

   iii. **Circular Error Probable (CEP).** For acquisitions within its radar horizon.

iv. **Target course estimation error.** Standard deviation (degrees) of error in estimating target's course.

v. **Target speed estimation error.** Standard deviation (knots) of error in estimating target's speed.

vi. **AIS capable?** – 'Yes' or 'No'. Does this surveillance vessel class have an Automatic Identification System receiver onboard.

vii. **Information latency.** The time delay between when the ship identifies and locates a target and when that information is used at the data fusion centre to update the RMP.

47. A SS Generator can be selected from a previously constructed set associated with the Regional View adopted and appended to the set of Generators employed with this Scenario, or a new Generator can be built by the user, appended, and saved for potential re-use.

48. If building a new SS Generator, the user will be able to click on the map display to define the Waypoint Zones for each (defined by 2 or more points on the map). Another option will be to enter latitude/longitude coordinates via keyboard. The zones defined must be convex in shape, and will be verified that they are indeed convex.

49. In fact, convexity is a common S6 model requirement for all elementary two-dimensional regions defined within the RV. Convexity is required to enable efficient determination that any given point in the RV is inside or outside this region. In the case of the Waypoint Zones, convexity ensures that the process of determining random points within the zones works smoothly as well. Annex G presents all the algorithms required to: verify a region is convex; calculate the region's area; determine if a point is inside or outside the region; or randomly select a point inside the region. All regions entered into the S6 model will be checked for convexity upon input, and the calculated area will be presented for information purposes to the user.

50. The key Measure of Effectiveness employed will be the ability of the system-of-systems to detect, classify, or identify those SS instantiated by a selected set of SS Generators, as specified by the user via parameter f. above. These will be recorded by waypoint zone, so the user should take care to ensure these waypoint zones are defined to represent useful regions (or lines) where certain levels of acquisition are desired to be achieved. See Chapter 6 for details on MOEs.

51. Also required will be a SS Generator preview capability. This capability will permit the user to graphically preview an existing Generator, a modified existing Generator, or a new one that has just been constructed. The preview will provide a textual list of the associated parameters to the user, along with a graphical depiction of the Waypoint Zones. It then will be able to provide two forms of display to permit visualization of the Generator's behaviour:

a. A preview of a small number (user selected) of randomly generated paths based on the parameters and Waypoint Zones entered.

b. A time-accelerated sequence of snapshots of SS positions over time, using the same display format as employed by the main simulation.

52. In both cases, the length of each sample path in both distance and time will be presented to the user.

53. As was the case with Figure 1, Figure 2 is provided as a notional example of what the GUI might look like for the SS Generator setup.

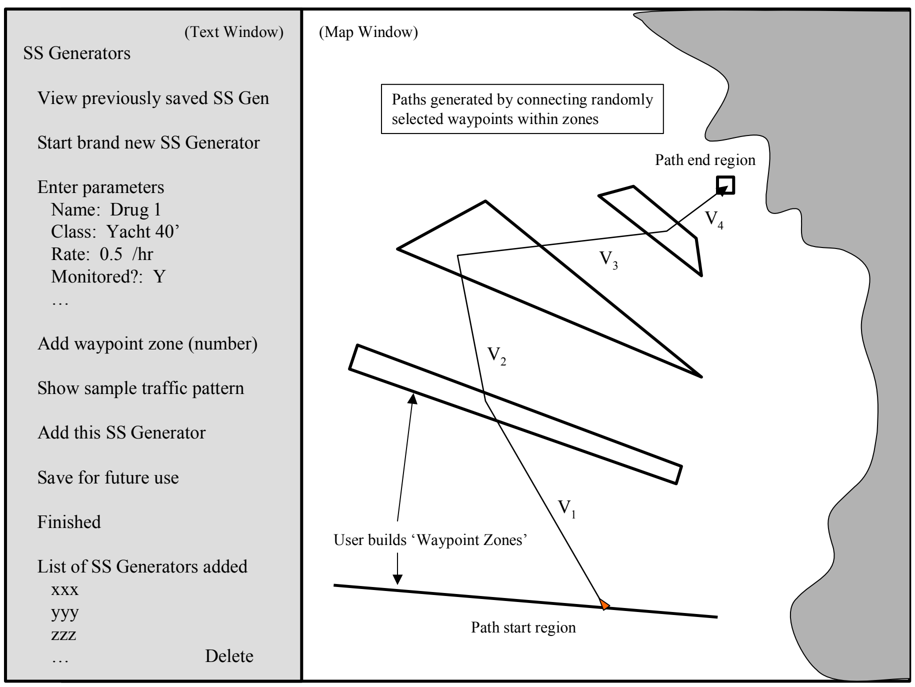

Figure 2. *Notional Graphical User Interface - SS Generator Setup*

4. SENSOR DATA OVERLAY GENERATORS

54. The term ‘sensor’ is defined here to represent a specific platform, carrying one or more physical devices for target acquisition and possibly including human operators as well. A sensor will operate on the background SS traffic at a given point in simulated time, producing a set (or layer) of information based on the performance parameters defined for that class of sensor.

55. Each Sensor Class will perform differently and will have event code uniquely written for that Class. Sensor Classes will include at least the nine types listed below. The S6 model will be designed and constructed so as to facilitate the addition of new sensor classes down the road, as required.

a. **P-AIR** – Pre-planned manned aircraft patrols

b. **R-AIR** – Reactive manned aircraft patrols

c. **UAV** - Unmanned Aerial Vehicle (UAV) patrols

d. **RAD** - Conventional ground radar stations

e. **SWR** – Surface Wave Radar (SWR) installations

f. **SAT** - Surveillance satellites

g. **GOV** – Navy, Coast Guard, or other government vessel patrols

h. **DF** – Electronic or acoustic direction finding systems

i. **SRS** – Self-reporting of vessels (SRS)

56. Note that this last item, SRS, does not include **Automatic Identification Systems (AIS)**. AIS information is available only to receivers within line-of-sight, so it is modelled within the constructs of other Sensor Classes. The SRS Sensor Class is designed to capture other self-reporting that might occur more broadly. Sensors with AIS receivers onboard will effectively fuse the AIS and sensor information before making the combined information set (taking the best values from both sources) available to the Data Fusion algorithm. The following global AIS parameters are defined and applied whenever surveillance aircraft (including UAVs), radars, or ships have been assigned AIS receivers. AIS hardware is assumed to be relatively consistent in technical accuracy, regardless of the classes of vessel on which the transponder is installed, so the following list of AIS parameters are assumed to be global parameters:

a. **Circular Error Probable (CEP)** – in nautical miles. This is the radius about the AIS-reported position that has 50% chance of including the actual ship’s position.

b. **Probability AIS transponder is operational at any point in time.** Any time an SD Generator checks to see if the AIS system onboard a SS is operational, this probability applies.

c. **Target course estimation error.** Standard deviation of the AIS-reported heading, in degrees.

d. **Target speed estimation error.** Standard deviation of the AIS-reported speed, in knots.

57. A 'SD Generator' is a user-defined instance of one of these Sensor Classes. The user will be able to use (and modify) a SD Generator saved from past simulation runs using the adopted Regional View, or will be able to construct a new SD Generator from scratch (and save for future use with this RV). SD Generators are attached to RVs because they often will have patrol regions defined within the Cartesian coordinate system of that RV.

58. The outputs of all SD generation events will be a list of targets with the following attributes for each 'datum', as shown in Table 1.

Table 1. *Sensor 'Datum' Record Provided*

'DATUM' INFORMATION ELEMENT
Time information was produced – This time may be in the past if there is information latency with the sensor. **Acquisition level** – detection, classification, or identification. If 'classification' is indicated, then an estimated Ship Class must be provided (which could be in error). A vessel's identity is simply its instantiation sequence number. **Estimated position** – coordinates in nautical miles in the Cartesian system. **Velocity vector estimate (optional)** - Not all systems will produce a velocity vector estimate. If provided, both heading (degrees from true north) and speed (knots) estimates must be given. **Radius of Positional Uncertainty (RPU_P)** – at the specified global Positional Confidence Level, *P*, defined as the radius of a circle centred on the estimated position that has probability *P* of including the actual target at this instant in time. **Target heading estimation error** – If a velocity vector estimate is provided, then the standard deviation associated with the heading must be provided. **Target speed estimation error** - If a velocity vector estimate is provided, then the standard deviation associated with the speed must be provided.

59. The Radius of Positional Uncertainty (refer to definition in Section 2.3) is a function of the inherent accuracy of the sensor, plus the latency of the sensor system in reporting the contact to the data fusion centre (combined with an assumed maximum speed of the target). Annex C provides an extensive description of the algorithms used to calculate RPU based on the foundation of the Circular Normal probability distribution. RPU_x (for any probability value x), CEP, and the σ parameter of the Circular Normal distribution are all easily related via the formulae in the annex.

60. For each SD Generator, the first parameter defined will be its Sensor Class. The event associated with each class is described below, outlining the associated parameters and internal logic applied.

61. Note that all SD Events will be scheduled for that point in time when the information they have produced is actually used in the Data Fusion algorithm. The requirement to handle latency – that is, the time delay between when the sensor information was gathered and when it was finally processed by the Data Fusion centre – means that any time a SD Event is scheduled, it must operate on the ground truth that existed at a point in time in the past: the current time *minus* the latency time. The need to be able to step back in time will require the simulation to maintain all vessel tracks, even those that might now be completed (vehicles will simply disappear after reaching the end of their paths). This feature also demands that early occurrences of any SD event cannot arise before the clock has passed the associated latency time, as the paths cannot be projected back into negative time.

62. In order to enable sensitivity analysis to be conducted on the set of information latency parameters entered for all sensors, a global parameter, the Information Latency Factor (ILF) can be specified. This multiplicative factor will be applied to all entered latency times, permitting the user to investigate the impact of having no time latency in reporting and processing information (ILF = 0), or the full entered values (ILF = 1), or anything in between.

63. Annex C describes how the sensor accuracy and information latency components of positional uncertainty are modelled within the context of the Circular Normal distribution.

64. The Data Fusion event is always triggered immediately following each SD Event.

4.1 Pre-Planned Aircraft Patrols (P-AIR Event)

65. The P-AIR event sends a patrol aircraft out to patrol a specified region, locating, identifying, and providing a velocity vector estimate for all vessels encountered. The user will specify the following parameters for a SD Generator in the P-AIR Class:

a. **SD Generator Name** – e.g. ‘P-AIR 1’

b. **Patrol region coordinates**. This will be a set of one or more convex polygons that the user will be able to define through the GUI or direct keyboard input and which outline the perimeter of the patrol region/sub-regions. Note that the overall region itself need not be convex, but each sub-region must (see Annex G). The sub-regions would probably be contiguous, but need not be. The GUI will present the sum of the areas of the convex sub-regions to the user, which will be useful in assuring that the overall region defines a reasonable patrol area, and is consistent with other regions as well.

c. **Patrol frequency**. Entered as the average time (hours) between patrols.

d. **Patrol recurrence mode.** There are two possibilities – ‘Regular’ or ‘Random’. If ‘Regular’ then the next patrol will always occur exactly the number of hours specified in c. after the previous patrol. If ‘Random’, then the next patrol will be scheduled according to a Poisson Process using the parameter in c. as the mean of the distribution (see Annex F).

e. **Probability of missing a target**. The patrolling aircraft may miss some targets in its patrol region.

f. **Circular Error Probable (CEP).** Radius of a circle (in nm) about the reported target position at the time of acquisition that has a 50% chance of including the actual target position.

g. **Target course estimation error**. Standard deviation (degrees) of error in estimating target’s course.

h. **Target speed estimation error**. Standard deviation (knots) of error in estimating target’s speed.

i. **AIS capable?** – ‘Yes’ or ‘No’. Does this aircraft class have an Automatic Identification System receiver onboard? Only transponding vessels in the surveillance region will be picked up.

j. **Information latency.** The time delay between when the aircraft identifies and locates a target, and when that information is processed at the data fusion centre.

66. When executed, a P-AIR Event will use global routines to determine the positions of all SS traffic targets at the current time *minus* the information latency time. It will then assess whether or not each target was within one of the convex polygons defining the patrol region (see Annex G).

67. The aircraft will be presumed to provide maximum information: location, identification, and a velocity vector estimate for all targets lying within the patrol region. Errors specified above will be randomized and incorporated into the reported information set (see Annex B for generation of random Normal deviates). If the aircraft has a AIS receiver onboard and the SS target’s AIS transponder is deemed to be functioning (random number draw against global probability value), then the CEP, target speed estimation error, and target course estimation error values used will be the minimum of the AIS global values and the P-AIR assigned values above. These minimum values will be used to generate the random Normal deviates.

68. Note that this type of event, which has a predominant ‘human eyeballs on the target’ character, does not permit false targets to be generated.

69. A SD Event always reports its information at a single instant in time (with a latency delay). For extended aircraft patrols this may not be the most realistic assumption. Depending on how the sensor data is being reported to the data fusion centre, the user may wish to instantiate extended aircraft patrols as a sequence of smaller sub-regions covered over time, rather than as a single large region covered all at once. Note that the

user would have to use the 'regular' patrol mode rather than the 'random' one to accomplish this.

70. The P-AIR event will also schedule its own next occurrence based on the recurrence mode (parameter d. above) and rate (parameter c.).

4.2 Reactive Air Patrols (RAPDC and R-AIR Events)

71. Before describing the R-AIR event, we must describe the inputs and behaviours associated with the Reactive Air Patrol Demand Check (RAPDC) event, which is run automatically after each Data Fusion event and is the only trigger for the R-AIR Event (R-AIR events do not reschedule themselves as most other sensor events do).

72. A set of convex geographic 'Trigger Regions' (TR) will be defined for the RAPDC Event. These will be set up via the Graphical User Interface (GUI) in the same fashion as the P-AIR regions. Each TR will be a single convex polygon that doubles as *both* the region of concern and the region to be patrolled. The user should build regions that are all comparable in size, representing reasonable air patrol areas. The GUI will provide calculated values of area to the user (as per Annex G).

73. The RAPDC Event will scan all Trigger Regions. Any TT in the RMP that has been located within that region, has not yet been identified, and has not triggered a R-AIR event in the past, will result in the scheduling of a R-AIR Event into that region, provided there is not already a patrol scheduled for that TR, and provided the limit for patrols during the current month of simulated time has not been exceeded.

74. Once initiated, the R-AIR event is very similar to the P-AIR Event. The R-AIR event's patrol region is the RAPDC event's TR, and will attempt to provide full information on all targets acquired within that region.

75. There can only be a single SD Generator in the R-AIR class. Events in this class will be created as determined by the RAPDC event. The user will specify the following parameters for the SD Generator in the R-AIR Class:

a. **SD Generator Name** – e.g. 'R-AIR' (there is only one in this class).

b. **Monthly patrol limit** – number of flights. Once this limit has been reached there will be no more flights scheduled until the next 30-day window of the simulation opens. The user can quickly check that the trigger/patrol region sizes and this limit on the number of flights combine to approximate any monthly flying hour quotas that might apply.

c. **Reaction time** – in hours, to respond to the request for a flight. This is measured from the time the request is initiated (RAPDC Event) until the aircraft is flying in the region (R-AIR Event is scheduled).

d. **Probability of missing a target.** The patrolling aircraft may miss some targets in its patrol region.

e. **Circular Error Probable (CEP).** Radius of a circle (in nm) about the reported target position at the time of acquisition that has a 50% chance of including the actual target position.

f. **Target course estimation error.** Standard deviation (degrees) of error in estimating target's course.

g. **Target speed estimation error.** Standard deviation (knots) of error in estimating target's speed.

k. **AIS capable?** – 'Yes' or 'No'. Does this aircraft class have an Automatic Identification System receiver onboard? Only transponding vessels in the trigger/patrol region will be picked up.

h. **Information latency.** The time delay between when the aircraft identifies and locates a target, and when that information is processed at the data fusion centre.

76. When executed, a R-AIR Event will use global routines to determine the positions of all SS traffic targets at the current time minus the information latency time. It will then assess whether or not each target was within the convex assigned trigger/patrol region (see Annex G).

77. The aircraft will be presumed to provide maximum information: location, identification, and a velocity vector estimate for all targets lying within the patrol region. Errors specified above will be randomized and incorporated into the reported information set (see Annex B for generating random Normal deviates). If the aircraft has a AIS receiver onboard and the SS target's AIS transponder is deemed to be functioning, then the CEP, target speed estimation error, and target course estimation error values used will be the minimum of the AIS global values and the R-AIR assigned values above. These minimum values will be used to generate the random Normal deviates.

78. Note that this type of event, which has a predominant 'human eyeballs on the target' character, does not permit false targets to be generated.

79. Annex C describes in detail how the information latency property is modelled.

4.3 Unmanned Aerial Vehicle Patrols (UAV Event)

80. Unmanned Aerial Vehicles, or UAVs, can be used to perform regular long-endurance patrols of a specified region, much like the P-AIR event but augmented with a *persistence* characteristic.

81. The UAV Event sends an air vehicle with onboard sensing to patrol a specified region, locating, possibly classifying or identifying, and possibly providing a velocity vector estimate for all vessels encountered. The user will specify the following parameters for a SD Generator in the UAV Class:

a. **SD Generator Name** – e.g. 'UAV 1'.

b. **Patrol region coordinates**. In the same fashion as for the P-AIR event, this is a set of one or more convex polygons that the user will be able to define, through the GUI or direct keyboard input, which define the perimeter of the patrol region/sub-regions.

c. **Patrol interval -** the time (hours) between the starts of regular patrols. The interval is not randomized, but is implemented as an exact interval between patrols (similar to P-AIR 'regular' patrols).

d. **On-station duration** – the on-station time for the UAV in hours. The UAV will regularly update the information provided throughout this on-station time. This parameter works in combination with e. below.

e. **Update interval** – in hours. While the UAV is on station, this is the time interval between updates provided to the Data Fusion algorithm. It should approximately represent the time required to re-survey its assigned region, and must be a non-zero value.

f. **Probability of missing a target.** The patrolling aircraft may randomly miss some targets in its patrol region every update interval.

g. **Circular Error Probable (CEP).** Radius of a circle (in nm) about the reported target position at the time of acquisition that has a 50% chance of including the actual target position.

h. **Level of target acquisition provided** – detection, classification, or identification. Manned aircraft are always assumed to provide identification information, but UAVs may operate only at higher altitudes and be incapable of achieving the resolution needed to classify and/or identify.

i. **Probability of classification error** – applied only if 'classification' is selected in h. above. If an error is generated, a randomly selected classification will be produced.

j. **Velocity vector estimated?** – Yes or No.

k. **Target course estimation error.** If j. is 'Yes', provides standard deviation (degrees) of error in estimating target's course.

l. **Target speed estimation error.** If j. is 'Yes', provides standard deviation (knots) of error in estimating target's speed.

m. **AIS capable?** – 'Yes' or 'No'. Does this UAV class have an Automatic Identification System receiver onboard?

n. **Information latency.** For each update, the time delay between when the UAV determines its information on a target, and when that information is processed at the data fusion centre.

82. When executed, a UAV Event will use global routines to determine the position of all SS traffic targets in the past at the current time *minus* the information latency time. It will then assess whether or not each target was within one of the convex polygons defining the patrol region (see Annex G).

83. Errors specified above will be randomized and incorporated into the reported information set (see Annex B). If the UAV has an AIS receiver onboard and the SS target's AIS transponder is deemed to be functioning during this update, then the CEP, target speed estimation error, and target course estimation error values used will be the minimum of the AIS global values and the UAV assigned values above. These minimum values will be used to generate the random Normal deviates.

84. The UAV Event will schedule its next update, unless it has run out of endurance (parameter d.), in which case it will schedule the first update in the next UAV patrol according to the patrol interval defined by parameter c.

4.4 Ground-Based Conventional Radars (RAD Event)

85. Ground-based radars can survey coastal regions, up to the limits imposed by line-of-sight, usually providing excellent accuracy.

86. The user will specify the following parameters in establishing a SD Generator in the RAD Class. Each physical radar installation will have its own SD Generator defined.

a. **SD Generator Name** – e.g. 'RAD 1'.

b. **Radar location coordinates.** The user will be able to specify through the GUI or via direct keyboard entry, including the option of entering latitude/longitude coordinates.

c. **Search azimuth limits.** The heading of the left edge and right edge of the search sector (using true north bearings in degrees within the Cartesian coordinate system).

d. **Maximum detection range by ship class.** If the radar was not horizon limited, this is the theoretical maximum range in nautical miles at which the radar could detect a vessel of each Ship Class.

e. **Radar altitude** - in feet above sea level. Radars will normally be situated on high ground to maximize their horizon over the water. Annex H presents the standard formula (see Skolnik [8]) for determining the radar horizon given the heights of the radar and the effective height of the ship. Although factors such as wind direction and sea state will influence radar horizon, these are not explicitly modelled. Any co-located AIS receiver is assumed to be at the same local height.

f. **Update interval** – in hours. This is the time between updates provided to the data fusion algorithm. This value cannot be zero.

g. **Mean Time Between Failures (MTBF)** – in hours. Annex F describes how to determine whether the radar system has failed since the last update was produced.

h. **Mean Time To Repair (MTTR)** – in hours. Annex F describes how to generate a random exponential time deviate based on the MTTR, yielding the time delay before the radar system will be operational again.

i. **Probability of missing a target**. The radar may miss some targets randomly during an update interval. It is assumed that each update is independent of the others when determining if a SS target is missed.

j. **Probability of generating false targets**. Values are expected to be low, so the user will specify the probability of 0, 1, or 2 false targets arising during any single update. The values must sum to 1. Again, it is assumed that all updates are independent of each other, so false targets do not persist. False targets will have a random range (up to radar horizon), bearing (within search sector), classification, and velocity vector (up to global maximum speed value) assigned.

k. **Circular Error Probable (CEP).** Radius of a circle about the reported target position at the time of acquisition that has a 50% chance of including the actual target position.

l. **Level of target acquisition provided** – 'detection' or 'classification'. Radar systems may be able to classify targets based on target strength and signature. Radars are assumed to be incapable of identification (unless they have an AIS receiver co-located and the target is transponding).

m. **Probability of incorrect classification.** If the answer above is 'classification' and there is no AIS info on a given SS target, then the radar system will err at a user specified rate. For misclassified targets, a randomly selected classification category will be assigned. It is assumed that subsequent updates are independent so misclassifications will not persist.

n. **Target course estimation error.** Provides standard deviation (degrees) of error in estimating target's course.

o. **Target speed estimation error.** Provides standard deviation (knots) of error in estimating target's speed.

p. **AIS capable?** – 'Yes' or 'No'. Does this radar class have an Automatic Identification System receiver co-located? If so, then this information will be merged with the radar information.

q. **Information latency.** For each update, the time delay between when the radar determines its information on a target, and when that information is processed at the data fusion centre.

87. Each RAD update event will determine which SS targets were within range of the radar at the current time *minus* the information latency time. It will introduce random

location errors according to the inherent accuracy and latency parameters (see Annex C), and will produce velocity estimates for all targets. Radars may or may not provide classification information on all targets, but if so they will have a classification error rate.

88. If the radar has an AIS receiver co-located with it, and the SS target's AIS transponder is deemed to be functioning during this update, then the identification, CEP, target speed estimation error, and target course estimation error values used will be the best provided between the two systems. These best values will be used to generate the random Normal deviates. Note that if the radar is down, then the AIS is assumed to be down as well. The RAD event will also check if there are AIS contacts that are outside radar detection range for that class of SS, but are still within the radar horizon and the radar's sector limits. If so, these sensor datums will be added to the SD list generated (using just the AIS global parameters, of course). This feature will permit stand-alone AIS stations to be modelled within the context of the RAD sensor.

89. Each RAD event schedules its next occurrence at a time in the future given by the update interval. Before it performs its update, it determines if the hardware has failed since the previous update (random draw as described in Annex F using the MTBF value), and if so, how long before it will be operational again (random draw as described in Annex F using MTTR value). If a failure is deemed to have occurred the event schedules its next occurrence for the current time plus the repair time. Note that the information latency time is already accounted for so there is no need to add it to the repair time.

4.5 Surface Wave Radars (SWR Event)

90. Surface Wave Radar is modelled similarly to conventional radar installations (RAD events), but with some additional attributes to reflect some of the performance differences. Each physical SWR installation will have its own SD Generator defined.

91. The primary difference with SWR is that it is not horizon limited. Using long wavelengths in the High Frequency (HF) band, the transmissions can propagate along the surface, taking advantage of the salinity of the ocean surface. The primary differences lie in how the maximum and minimum ranges vary over time. HF wave propagation is very much dependent on ionospheric conditions and clutter. It varies by time of day and varies from day to day.

The following parameters will be specified for a SWR SD Generator:

a. **SD Generator Name** – e.g. 'SWR 1'

b. **SWR location coordinates**. The user will be able to specify through the GUI or via direct keyboard entry, including the option of entering latitude/longitude coordinates.

c. **Search azimuth limits**. The heading of the left edge and right edge of the surveillance sector (using true north bearings in degrees within the Cartesian coordinate system).

d. **Minimum detection range** – in nm. SWR usually have an inner radius (nm), inside which targets cannot be detected.

e. **Maximum daytime detection range** – in nm, by ship class and by aspect (two values). Radar cross-section is important for this class of sensor. A value for beam aspect and for head-on/tail-on aspect is specified for each ship class. Aspect values will be linearly interpolated based on the actual aspect angle being presented to the target.

f. **Standard deviation of maximum daytime detection range** – in nm. HF wave propagation varies from day to day. A random Normal deviate is drawn at the start of the day and this correction is applied throughout the day

g. **Maximum nighttime detection range scaling factor.** This multiplicative scaling factor applies to convert all daytime maximum detection ranges to night time values. The user will specify two global parameters: the number of hours of daylight per day and the time of day at sunrise.

h. **Update interval – in hours.** This is the time between updates provided to the data fusion algorithm. This value cannot be zero.

i. **Mean Time Between Failures (MTBF)** – in hours. Annex F describes how to determine whether the SWR system has failed since the last update was produced.

j. **Mean Time To Repair (MTTR)** – in hours. Annex F describes how to generate a random exponential time deviate based on the MTTR, yielding the time delay before the SWR system will be operational again.

k. **Probability of missing a target.** The radar may miss some targets randomly during an update interval. It is assumed that each update is independent of the others when determining if a SS target is missed.

l. **Probability of generating false targets.** Values may be higher than for normal radar systems, so the user will specify the probability of 0, 1, 2, … , 5 false targets arising during any single update. The values must sum to 1. Again, it is assumed that all updates are independent of each other, so false targets will not persist. False targets will have a randomly selected range (uniformly distributed between minimum and the applicable maximum), bearing (random within search sector), and velocity vector (up to global maximum speed value with random heading) assigned.

m. **Circular Error Probable (CEP)** – in nm. Radius of a circle about the reported target position at the time of acquisition that has a 50% chance of including the actual target position.

n. **Velocity vector estimated?** – Yes or No. User selects SWR ability to track between updates and provide a velocity vector estimate.

o. **Target course estimation error.** If 'Yes' in n. above, provides standard deviation (degrees) of error in estimating target's course.

p. **Target speed estimation error.** If 'Yes' in n. above, provides standard deviation (knots) of error in estimating target's speed.

q. **AIS capable?** – 'Yes' or 'No'. Does the SWR class have an Automatic Identification System receiver co-located? If so, then this information will be merged with the radar information.

r. **AIS receiver height** – in feet above sea level. If the SWR is deemed AIS capable, the height of the AIS receiver must be specified (enables horizon to be calculated).

s. **Information latency** – in hours. For each update, the time delay between when the SWR determines its information on a target, and when that information is processed at the data fusion centre.

92. Each SWR update event will determine which SS targets were within the range limits of the radar at the current time *minus* the information latency time. While the minimum range constraint is always the same, the maximum range constraint will vary according to the day, the time of day, the class of target, and its presented aspect angle. Annex I provides the details of how this maximum range value is calculated.

93. The event will introduce random location errors according to the inherent accuracy and latency parameters (see Annex C), and will produce velocity estimates for all targets if assigned that capability. It may miss targets and may generate a number of false targets.

94. If this SWR installation is designated as AIS capable, and a SS target is: within the SWR search azimuth limits, within the radar horizon (calculated via Annex H); has been assigned an AIS transponder; and that AIS transponder is currently functioning, then the AIS information will be blended in with the SWR information. The SWR minimum range restriction does not apply to AIS acquisitions. The identification, CEP, target speed estimation error, and target course estimation error values used will be the best provided between the two systems. These best values will be used to generate the random Normal deviates. Note that if the radar is down, then the AIS is assumed to be down as well.

95. Because of the vagaries of HF propagation, SWR is deemed capable of providing only a detection capability (in the absence of AIS augmentation).

96. Each SWR event schedules its next occurrence at a time in the future given by the update interval. Before it performs its update, it determines if the hardware has failed since the previous update (random draw as described in Annex F using the MTBF value), and if so, how long before it will be operational again (random draw as described in Annex F using MTTR value). If a failure is deemed to have occurred the event schedules its next occurrence for the current time plus the repair time. Note that the information latency time is already accounted for so there is no need to add it to the repair time.

4.6 Satellites (SAT Event)

97. The S6 model will have the ability to simulate the coverage of the Regional View provided by constellations of surveillance satellites. The modelling challenge is to represent this coverage realistically, yet in as simple a way as possible. Some orbital parameters will be essential to represent. These are: the orbital inclination; the period; and the sensor's swath width. The orbital inclination is the angle that the satellite ground track makes with the equator as it passes overhead from south to north (i.e. is 'ascending'). The period is the time it takes to complete a single orbit of the earth.

98. Many surveillance satellites like RADARSAT, SPOT, etc. operate in circular, sun-synchronous orbits. These are special near-polar orbits. The extra girth of the earth at the equator causes satellites in these orbits to precess at about 1 degree per day, which results in them maintaining the same position with respect to the sun as the year progresses. The dawn-dusk orbit is particularly attractive for solar power generation as it results in the satellite never being in the earth's shadow.

99. A useful property of sun-synchronous orbits is that the points they pass over are always at the same local time (assuming continuous time zones) while ascending and 12 hours different while descending. This simple relationship between local time of day and satellite longitude as the earth spins beneath it will enable our modelling approach to be simplified as well. We will tie time and longitude together. This will be accurate for sun-synchronous orbits, but will be missing a small correction factor for other orbits.

100. The RADARSAT website [9] lists the following orbital parameters for RADARSAT 1 and 2: circular orbit; orbital inclination 98.6 degrees; altitude 431 nm; period of 100.7 minutes (1.6783 hrs); ascending time of 1800 hours local, and descending time of 0600 hours local.

101. Each satellite in a constellation will have its own SD Generator defined. It is assumed that satellite sensors will provide detection or classification information only, and will *not* have the capability to estimate a velocity vector. The user will specify the following parameters for a SD Generator in the 'SAT' class.

a. **SD Generator Name** – e.g. 'SAT 1'

b. **Orbital inclination** – in degrees. This is the angle the satellite makes with the equator as it crosses the equator from south to north. It is identically the maximum latitude (north and south) that the satellite will pass over. Sun-synchronous orbits are typically around 98 degrees inclination.

c. **Orbital period** - in hours. How long the satellite takes to complete one orbit of the earth.

d. **Sensor swath width** – in nautical miles. Although the detailed calculations in Annex J assume the swath will be centred on the ground track, the calculations are valid for any swath offset as long as the RV is not at extreme northern or southern latitudes in relation to the orbital inclination.

e. **Ascending local time** - between 0 and 24 hours. This is the local time on the ground whenever the satellite passes overhead on the ascending half of its orbit. The descending local time is this value ±12 hours, whichever value is positive and less than 24 hours.

f. **Time the satellite first crosses the central latitude ascending** – in hours, between zero and the orbital period, T. The central latitude and longitude define the centre of the Regional View, and simulation time-of-day is assumed to be in the time zone of the RV at this point. The first descending time is calculated from this value using the Annex J formulae. This parameter can be specified in one of two ways:

   i. **Randomly** – the simulation will select a random uniform value on the interval [0,T].
   ii. **User specified** – this feature enables satellites in a constellation to be set up relative to each other.

g. **Circular Error Probable (CEP).** Radius of a circle (nm) about the reported target position at the time of acquisition that has a 50% chance of including the actual target position.

h. **Level of target acquisition obtained** – detection or classification. It is assumed that satellites will not be able to identify ships, but may have sufficient resolution to classify them.

i. **Probability of incorrect classification.** If the answer above is 'classification', then the system will err at a user specified rate. For misclassified targets, a randomly selected classification category will be assigned. It is assumed that subsequent updates are independent so misclassifications will not persist.

j. **Probability of missing a target.** The satellite's sensor may miss some targets randomly during an update interval. It is assumed that each satellite pass is independent of the others when determining if a SS target is missed.

k. **Probability of generating false targets.** The user will specify the probability of 0, 1, 2, … , 5 false targets arising during any single pass. The values must sum to 1. Again, it is assumed that all updates are independent of each other, so false targets will not persist.

l. **Information latency.** For each pass, the time delay between when the satellite determines its information on a target (nominally the time at which it crosses the central latitude), and when that information is processed at the data fusion centre.

102. Annex J provides a detailed description of how the above parameters are used to determine the time of the next ascending or descending pass over the Regional View, and how to determine the coordinates and orientation of the coverage parallelogram. Figure 1 provides a simplistic illustration of a satellite pass over the RV.

103. When a SAT event is executed, the event will determine the proper position and orientation for the coverage parallelogram and the position of all SS targets at the time of the pass (the current time minus the information latency time). It will determine which

targets lie within the coverage zone using the convex region algorithms of Annex G (a parallelogram is always convex). The event will act on the above inputs, generating random positional errors according to the specified CEP, missing some targets randomly, misclassifying others (if assigned the ability to classify) randomly, and generating a random number of false targets, each with random properties. As mentioned before, satellite sensors are assumed to be unable to produce velocity vector estimates.

104. Satellites are assumed *not* to be AIS capable. However, defining another SS Generator of the SAT class with the identical orbital parameters and assigning it a suitable swath width to represent AIS coverage could simulate this capability.

105. The number of false targets will be determined by random number draw. These false targets will have a randomly selected location within the coverage parallelogram (see Annex G methods). We use the full parallelogram to ensure a consistent rate of false target generation, but the parallelogram may not overlap the entire RV. Hence, only those false targets lying within the RV will be passed on to the Data Fusion algorithm.

106. The event will then schedule its next pass over the region. Using the logic outlined in Annex J, the event will determine the next time at which the satellite passes over some part of the RV, and whether it is on an ascending or descending portion of the orbit. It then will schedule the next event for this SD Generator for the time the satellite is to cross the central latitude *plus* the information latency time, and noting whether it will be an ascending or descending pass.

4.7 Government Vessel Patrols (GOV Event)

107. Although surface ships travel very slowly, they have the ability to combine extended presence over time and an identification ability that may be unique.

108. Special SS Generators can be assigned the ability to create ships that conduct surveillance themselves, becoming SD Generators. Once instantiated, the vessels will regularly report identity, location, and velocity vector information on all other SS targets within their radar horizon as they follow their assigned path. The first report (GOV event) is scheduled by the SS Generator for the instantiation time plus the update interval plus the information latency time. Subsequent updates will be scheduled regularly, as defined by the update interval parameter, until the ship reaches the end of its path.

109. These ships are likely to have an integral helicopter to assist in the localization and identification. Surveillance vessels without helicopters can be assumed to deviate off their generated path in order to identify targets, but ‘officially’ they stay on the generated path. The leg speed values assigned for the SS Generator should reflect the net speed the vessel would be able to maintain as it surveys its region.

The GOV Event inherits the following parameters from the applicable SS Generator (see Chapter 3):

a. **SD Generator Name** – e.g. ‘GOV 1’

b. **Update interval.** Time (in hours) between surveillance updates provided to the Data Fusion algorithm. This value should match the patrol speed. If it is too large targets may slip through between updates, if it is too short then it increases computation time.

c. **Probability of missing a target.** The ship may miss some targets within its radar horizon every update.

d. **Circular Error Probable (CEP).** For acquisitions within its radar horizon.

e. **Target course estimation error.** Standard deviation (degrees) of error in estimating target's course.

f. **Target speed estimation error.** Standard deviation (knots) of error in estimating target's speed.

g. **AIS capable? –** 'Yes' or 'No'. Does this surveillance vessel class have an Automatic Identification System receiver onboard?

h. **Information latency.** The time delay between when the ship identifies and locates a target and when that information is processed at to the data fusion centre.

110. Each GOV update event will use global routines to determine which SS targets were inside the ship's radar horizon at the current time *minus* the information latency time. It will attempt to identify all targets inside this horizon, but each target has a random number drawn and compared to parameter b. to determine if it is missed during this update. The event will then introduce random location and velocity vector errors according to the parameters above, as described in Annex B.

111. If the surveillance vessel has an AIS receiver onboard and the SS target's AIS transponder is deemed to be functioning during this update, then the CEP, target speed estimation error, and target course estimation error values used will be the minimum of the AIS global values and the ship's assigned values above. These minimum values will be used to generate the random Normal deviates.

112. Identification of all targets is assumed (except for those missed by application of c. above), so the generation of false targets does not apply.

113. Finally, the GOV event reschedules itself for the current time plus the update interval (the information latency factor is already accommodated) if it has not reached the end of its path.

4.8 Direction Finding Systems (DF Event)

114. Ships often will rely on high frequency (HF) band radios for over-the-horizon communications. Stations set up to intercept these signals can determine a bearing from the station to the emitting ship. With multiple stations the ship's position can be cross-fixed. Using intelligence means, the system may be able to determine the classification

or even the identity of the vessel from the content of the radio signals. Of course, HF direction finding (HFDF) systems rely on the target cooperatively emitting a signal.

115. Also included in this category are fixed passive sonar systems. Sound travels exceptionally well in water, enabling ships to be detected at long range. Multiple receiving stations, which usually consist of underwater arrays of hydrophones hard-mounted to the seabed with the capability to perform complex processing of the acoustic signals, can cross-fix the sound source. Using intelligence means, an acoustic signature can be like a fingerprint in enabling it to be possibly classified or even identified. Unlike the HFDF system, the ship does not have to be cooperative to be detected. As long as it is moving it will be generating an acoustic signature.

116. It is assumed that a cross-fixed location may be determinable with these systems, but that no velocity vector information is obtainable.

117. The following parameters are defined for each SD Generator in the DF class.

a. **SD Generator Name** – e.g. ‘DF 1’.

b. **Update interval** – in hours.

c. **List of stations and their coordinates** – in the Cartesian coordinate system, although values can be entered as latitude/longitude pairs. These stations are the only items in the simulation that are allowed to lie outside the Regional View. At least two stations must be listed in order to enable cross-fixing.

d. **Azimuth fixing accuracy** – in degrees. The standard deviation of the angular error in fixing the bearing from a station to an emitter.

e. **HF signal emission probability during an update period** - by SS Class. Updates are assumed to be independent so transmission outages will not persist. Value would be set to 1.0 for passive sonar systems. This parameter must be related to the length of the update interval, so that is why it is not specified as a SS Class parameter.

f. **Maximum detection range -** in nm, by SS Class. It is assumed that HFDF systems have no detection range limitations (user enters a very large value), but passive sonar might. This parameter has to be related to the capability of the passive sonar system, so that is why it is not specified as a SS Class parameter.

g. **Maximum detection range at zero speed** – in nm, by Ship Class. It is useful to be able to represent reduced acoustic detection ranges if targets are travelling slower (and producing less acoustic energy). The actual maximum range used will be linearly interpolated between g. and f. depending on the fraction of maximum ship speed that the ship is currently running at.

h. **Probability of classification and identification**. Intelligence can assess HF transmission content or acoustic signature to possibly give classification or identification information. Two probabilities are given, one for identification and one for classification only. They cannot sum to more than 1. Simple detection occurs with probability 1 minus the sum of the two.

i. **Probability of misclassification.** If a random draw against the probabilities in h. determines that the SS target has been classified only, then there is a probability of a classification error. Identification is presumed to be declared only when certain, so there is no identification error modelled.

j. **Information latency.** The time delay between when the system locates and possibly identifies a target and when that information is processed at the data fusion centre.

118. Each DF update event begins by determining the actual position and speed of all SS targets at the time the information was collected: the current time *minus* the information latency time. It draws random numbers to determine if targets were emitting during this update interval (parameter e.). For emitting targets, it then determines whether each station is within the maximum range (interpolated between parameters g. and f. using SS actual speed at that time).

119. The event processes each emitting SS target in turn that has at least two stations within range. The actual bearing (in the Cartesian space) from each station to the target is calculated. A random Normal deviate is then applied to each, generating an estimated bearing to the target. Using the algorithm detailed in Annex K, the event then finds the pair of stations that has the least combined error in fixing the emitter's location. This process defines a region that has the probability P (the global Positional Confidence Level) of including the actual SS target. This region is approximately parallelogram shaped, and is converted to a circle of equal area.

120. Note that the algorithm uses only the information from the two best stations and discards the information from the other stations. This is done for the sake of keeping the algorithm relatively simple.

121. The DF event does not provide a velocity vector estimate.

122. The DF event will finally determine the level of acquisition - detection, classification, or identification – as determined by a random draw against the probabilities specified in h. above. If classification is selected, then there is a random number drawn to determine if it will be mis-classified.

123. Before calling the Data Fusion algorithm, the DF event reschedules itself for the current time plus the update interval.

4.9 Self-Reporting Systems (SRS Event)

124. If cooperative vessels report their position, identity, and intentions, this may help production of the RMP. Such vessels are unlikely to be the 'rogue' threats that the system-of-systems is ultimately trying to identify and locate, but having full, current information on the rest of the traffic may help considerably.

125. The self-reporting we are considering here is in addition to that reported via Automatic Identification Systems (AIS). AIS transponders onboard SS targets can only be picked up by receivers with direct line-of-sight to the target. For this reason, AIS information is integrated into the outputs of other sensors that might also have an AIS receiver onboard, as has been described in the previous sections in this chapter. We wish to have some mechanism to simulate the self-reporting of vessels (presumably via long range communications means) independently of how they are otherwise being surveyed. These cooperative vessels are assumed to provide full information – identity, location, and velocity vector.

126. A single global SD Generator of the SRS class can be established, with the following parameters:

a. **SD Generator Name** – e.g. 'SRS' (there is only one generator in this class).

b. **Update interval** – in hours. The time between updates provided by the self-reporting event, by ship class.

c. **Circular Error Probable (CEP)** – in nautical miles. The positional error in the reported position at the time it was reported. All classes of SS are assumed to have the same accuracy, as presumably all will be operating with Global Positioning System (GPS)-based navigation systems.

d. **Target heading estimation error – in degrees.** Standard deviation of error in the self-reported heading.

e. **Target speed estimation error – in knots.** Standard deviation of error in self-reported speed.

f. **Information latency** - in hours. For each update, the time delay between when the information is reported and when that information is processed at the data fusion centre.

127. At each update, the positions of all SS will be determined at a point in time in the past equal to the current time minus the information latency time. Regardless of its location within the Regional View, each SS that adopted a self-reporting policy (SRP) upon instantiation will have a random number applied to determine whether it is adhering to its SRP for this update (as per the probability assigned for that ship class). If it is, then its identity, and estimates of its location and velocity vector will be generated using the randomization principles described in Annex B applied with the error parameters above. This SD overlay will then be provided to the Data Fusion algorithms.

128. All SS that double as surveillance vessels (as per descriptions in Chapter 3 and Section 4.7) will be mandatory self-reporters.

129. The SRS event will then schedule itself to reoccur at the current time plus the update interval (the information latency factor is already accounted for).

This page intentionally left blank.

5. UPDATING THE RECOGNIZED MARITIME PICTURE

130. The execution of each Sensor Data event will produce an overlay of information – a list of new acquisitions with the information from Table I provided for each: the time at which the information was generated, the level of acquisition (and estimated classification if that level is indicated), the estimated location, the estimated error in location (Radius of Positional Uncertainty), and optionally the estimated velocity vector, and associated error estimates for the speed and heading.

131. The Recognized Maritime Picture consists of a list of Tracked Targets that have the identical set of parameters. The only difference is the time parameter represents the last time this TT was updated with new information. The philosophy is simple: combine the new SD overlay with the existing RMP to produce an updated RMP. Then let the clock move forward to the next event.

132. The heart of the S6 simulation is this updating or 'data fusion' mechanism. The objective is to eventually have a number of data fusion algorithms available to plug in at this point. The contractor will provide the 'roughed in plumbing' to enable other any number of data fusion routines to be inserted into the code and selected by the user at the start of a run. For the initial implementation we will specify a simple default data fusion algorithm.

133. Note that in application the objective will always be to model a *realistic* fusion process, not necessarily a *perfect* process. The effectiveness of various sensor combinations will not be truly represented if the fusion of that data is unrealistically simulated. Data fusion algorithms that match the actual processes used to generate the RMP in the Maritime Forces Atlantic (MARLANT) and Maritime Forces Pacific (MARPAC) regions will be logical follow-on user developments to complement this default algorithm once a functional S6 model has been constructed.

134. Information latency is an important property to consider while developing and maintaining a RMP, and it is a challenge to model. Surveillance information that arrives after some delay may not be a problem if the data fusion system can back up its process to the point in time when the information was fresh, integrate that information, and then re-integrate the information that arrived after that point in time. But if the fusion process has no time rollback ability, late information may quickly become useless. The S6 Model will permit users to establish where between these two end points on this spectrum they would like to operate. The default data fusion algorithm itself has no ability to go back in time to re-integrate stale information, but the user can select any set of information latency times desired to simulate any point between none and perfect rollback (all latency times would be set to zero). In fact, the simulation will have a global information latency factor, or ILF, which allows the user to scale all entered information latency times and easily perform sensitivity analysis on latency.

5.1 Default Data Fusion Algorithm

135. The default algorithm will seek to match each Sensor Datum in the overlay with a suitable Tracked Target in the RMP using an appropriate metric to determine best

matches. Matches are always one-to-one; that is, the algorithm will not try to match multiple SDs to an existing TT or vice versa. SDs that don't find a match will be injected into the new RMP as fresh targets. TTs that don't find a match will simply continue on in the new RMP as un-updated targets.

136. The following multi-step process will be followed.

137. **Step 1.** For each SD in the new overlay calculate the estimated current position and the Radius of Positional Uncertainty at the √P confidence level, $RPU_{\sqrt{P}}$ (where P is the global Positional Confidence Level), using the algorithm detailed in Annex C. This algorithm accounts for the information latency time and for any Heading Consistency Factor applicable.

138. **Step 2.** For each TT in the current RMP, calculate the estimated current position and $RPU_{\sqrt{P}}$ using the algorithm detailed in Annex D. This algorithm accounts for elapsed time since the TT was last updated and for any HCF applicable.

139. Note that the HCF employed in these first two steps permits predictability in future target positions and has properties analogous to a Kalman Filter.

140. **Step 3.** Cull the RMP of stale targets, removing all TT that have exceeded a global maximum value for $RPU_{\sqrt{P}}$.

141. **Step 4.** Identify all SD/TT pairs that are not compatible based on conflicting identification or classification information. That is, the TT carries identification but the SD identification doesn't match, or the SD classification doesn't match that of the identified TT, or the TT is classified but doesn't match the classification of the identified or classified SD.

142. **Step 5.** For each feasible combination of SD and TT, calculate the area of intersection of the two circles and the coordinates of the centre point of the intersection region, as detailed in Annex E.

143. **Step 6.** Calculate the fraction that the intersection area occupies of the total area of the TT circle. This will be the 'goodness of match' metric used to pair new SD to existing TT on a 1-to-1 basis.

144. This metric is superior to simply using the area of intersection itself, or the fraction that the intersection area occupies of the total area of the SD circle. TTs that have a very large circle because they have not been updated recently may well enclose many SD circles in their entirety, and it would not make sense to assign a SD to that TT if there was another recently updated TT with a very small circle that also had substantial (but not complete) intersection. Thanks to Dr. Yaw Asiedu for recommending this metric.

145. Ignore all SD/TT pairs whose circles do not intersect, then sort the remaining SD/TT pairs in decreasing order of this intersection fraction metric.

146. Repeat the following three steps until this list is fully emptied.

147. **Step 7.** Select the top item remaining on the list and declare this SD as a match to this TT.

148. **Step 8.** Copy the TT into the new RMP, updating the level of acquisition, position, velocity vector, and associated error parameters as follows:

- Level of acquisition. Assign the maximum level of acquisition from the SD and its matching TT to the new TT (where identification ranks higher than classification which ranks higher than detection).

- Position and positional error. Assign the new TT position to be the calculated centre of the circle intersection region as per Annex E. Since each circle had probability $\sqrt{P}$ of including the actual target, the intersection region is declared to have $(\sqrt{P})(\sqrt{P}) = P$ probability of including the target. Assign the RPU_P value to be the radius of the circle with area equal to the intersection area. See equation (E14) of Annex E.

- Velocity vector and errors. Compute the time-differenced velocity vector using the straightforward formulas in Annex L. Assign this velocity vector and its associated global speed and heading error parameter values to the new TT in lieu of the vector estimate of the SD if:

  i. The sensor did not generate a velocity vector estimate, or
  ii. The sensor's information latency time exceeds the time interval since this TT was last updated (rendering the new sensor datum as too stale regardless of its accuracy), or
  iii. The product of the estimated speed, the speed error standard deviation, and the heading error standard deviation for the time-differenced calculation is less than the product of those three quantities for the Sensor Datum. Refer to Annex L for additional details and discussion.

- Update the 'last update' time. Reset the last update time for the new TT to the current time.

149. **Step 9.** Remove all remaining SD/TT pairs from the list that involve this SD or this TT. Go back to Step 7 until the SD/TT list is exhausted.

150. **Step 10.** Once the list is exhausted, there may well remain SD that were not used. If so, declare each of these as a new TT in the RMP, carrying over all the SD information to the TT. Set the 'Last Update' time to the current time. Note that we do *not* subtract the information latency time from the current time here, as possible movement during that time interval has been accommodated in updating position and velocity.

151. **Step 11.** Also, there may be old TTs that were not updated. Transfer all these old TTs into the new RMP unchanged. As their 'Last Update' time gets older the positional uncertainty will grow and these targets will eventually get culled when it exceeds a global specified value.

152. Now the RMP has been updated.

This page intentionally left blank.

6. OUTPUT MEASURES OF EFFECTIVENESS (MOE)

153. As the simulation executes (towards its specified simulation time limit), it will record success against target acquisition criteria defined by the user. When execution is completed, it will present these results to the user. This information should be easily exportable into a spreadsheet such as Microsoft Excel.

154. During setup, the user specified which Surface Ship Generators are to be monitored. For each 'monitored SS', the time at which that ship was first detected, first classified (correctly), and first identified will be recorded. The Sensor Data Generator delivering that acquisition will also be recorded. Times when track was lost on the monitored SS and times of subsequent re-acquisition will also be recorded. Tracks are declared 'lost' when a TT (and the associated SS on which it was based) is culled due to an excessive RPU value.

155. This function should be easily accomplished within the different sensor events. When creating the Sensor Data overlay the event will know the underlying 'ground truth' and variables can be maintained for each SS to indicate if that target is currently being tracked and the highest level at which it has previously been acquired. If a change in acquisition status has occurred, the time of the acquisition will be recorded (the time at which it was 'actionable', so the actual time of detection plus the information latency time will be the recorded time, which is usually the current time when the event is executing). Of course, identification implies classification and detection, and classification implies detection. When contacts are dropped from the RMP for having excessively large RPU values, these times will be recorded as well.

156. But a string of times noting when acquisition was gained and lost is really only intermediate output. The user will want to know what the acquisition status was when each monitored SS reached their critical waypoints. When a monitored SS is instantiated its path is defined, and the future times at which the SS will reach its waypoints are known. The simulation will compare these waypoint times to the set of times accumulated during the simulation run to produce a one-line report on each instance of a monitored SS. It will also summarize the waypoint performance of the system-of systems against this SS target type in percentage terms. Table 2 illustrates the type of output that might be generated.

Table 2. *Example of Possible Output of MOEs*

SS Gen	Start	1st Det	by	1st Cls	by	1st ID	by	WP1	WP2	WP3	WP4	WP5	End
Rogue 1	8.11	9.02	UAV 1	12.20	DF 3	14.66	GOV 6	-	-	D	C	I	I
Rogue 1	15.44	30.22	P-AIR 1	30.22	P-AIR 1	30.22	P-AIR-1	-	-	-	I	-	D
Rogue 1	30.01	35.78	SWR 2	40.20	R-AIR	40.20	GOV 6	-	-	D	-	D	I
Rogue 1	32.74	-1.00		-1.00		-1.00		-	-	-	-	-	-
Rogue 1	66.31	67.33	SAT 3	-1.00		-1.00		D	D	D	-	-	D
Rogue 1	76.97	80.36	SWR 2	95.55	RAD 7	-1.00		-	-	D	D	D	C
Rogue 1	85.10	87.29	SAT 1	96.83	UAV 3	101.20	R-AIR	D	-	C	-	D	I
Pct Det								28.6	14.3	71.4	42.9	57.1	85.7
Pct Cls								0.0	0.0	14.3	28.6	14.3	57.1
Pct ID								0.0	0.0	0.0	14.3	14.3	42.9

SS Gen	Start	1st Det	by	1st Cls	by	1st ID	by	WP1	WP2	WP3	End
Rogue 2											
…											

REFERENCES

1. Fisher, M., *A Survey of ORAE Papers Pertaining to issues of Maritime Surface and Aerial Surveillance*, DMOR Staff Note 91/14, Directorate of Maritime Operational Research, November 1991, Unclassified.

2. Mason, D.W., *Analysis of National Surveillance Capabilities: Assessing Performance Against Air and Surface Targets*, ORAE Project Report PR677, Operational Research and Analysis Establishment, July 1994, Unclassified.

3. Fong, V., *A Simulation Study of Multi-Sensor Maritime Surveillance Using SIMLAB*, DRDC CORA Technical Report TR 2005-21, Maritime Operational Research Team, August 2005, Unclassified.

4. Dickinson, R., Martel, S., and Jesion, A., *Measures of Performance and Effectiveness for Surface Surveillance*, Project Report PR 1/97, Maritime Forces Atlantic Operational Research Division, August 1997, Unclassified.

5. Bourdon, S., Dore, LCdr S., Fong, V., and Gauthier, Y., *Defining and Selecting Metrics for Intelligence, Surveillance, and Reconnaissance*, DOR(MLA) Research Note RN2004/08, September 2004, Unclassified.

6. Lindsey, G.R., *Map Projections*, DSAG Seminar, Undated, Unclassified (copy available upon request).

7. Emond, E.J, *Notes on the Circular Normal Distribution*, unpublished note, Directorate of Mathematics and Statistics, Operational Research and Analysis Establishment, 29 August 1978, Unclassified (copy available upon request).

8. Skolnik, M.I., *Introduction to Radar Systems, Third Edition*, McGraw-Hill, 2001.

9. RADARSAT web site at www.radarsat2.info.

10. Mason, D.W., *Display of Concrete Objects With Hidden Edge Removal Option*, DAOR Staff Note 81/5, Directorate of Air Operational Research, September 1981, Unclassified.

11. Abramowitz, M., and Stegun, I.A., *Handbook of Mathematical Functions*, Dover Publications Inc., November 1970.

12. Parzen, E., *Stochastic Processes*, Holden-Day Publishing, 1967.

This page intentionally left blank.

Annex A
Map Projections

157. The S6 model will be simulating surveillance across a broad geographic region, one that spans hundreds of nautical miles in breadth, if not a thousand or more. At this scale, the argument to use the planet's natural spherical coordinate system – i.e. latitude and longitude, - gets stronger and stronger. The advantage of the Cartesian (i.e. flat earth) coordinate system is its simplicity. It is so much easier to work the mathematics if the earth can be considered flat. And since our geographic window into the region is a computer screen, which is effectively a flat, two-dimensional surface anyway, we have made the firm decision to use the Cartesian system as our primary coordinate system.

158. We require the ability to relate the spherical real world to the two-dimensional simulation world. Key geographic features or sensor locations will have to be accurately transferable onto the Cartesian plane. Indeed, if the contractor's choice was to use vector-drawn maps operating on vector coastline and other feature data, all of the geographic content would have to be accurately transferable. This will require the ability to convert from spherical to Cartesian coordinates when required (although the reverse conversion is not expected to be required).

159. A suitable map projection needs to be identified. Lindsey [6] gives an overview of the realm of possible projections that might be considered. As the reference states, "there is no best projection". All have distortions of some kind – angles, areas, distances. It depends on what properties you wish to keep and what you are willing to sacrifice. It boils down to finding one that produces reasonable looking images and has reasonably direct mathematics for conversion.

160. The orthographic projection is a reasonable choice. This is the projection of a sphere onto a plane from a viewpoint at infinity, at the zenith above a specified point on the earth's surface. The advantage of this projection is the naturalness of the view (we see the moon from earth as basically an orthographic projection). The distortions are minimal near the 'zenith' point and get larger as distance from that point on the earth's surface increases. Long distances, especially near the edges of the Regional View, will be shortened slightly.

161. The mathematics of the orthographic projection will be presented below, should the contractor wish to adopt this projection.

Mathematics of the Orthographic Map Projection

162. Mason [10] presents a full description of the mathematics behind orthographic and perspective projections. The process of performing an orthographic projection of a sphere onto the plane is summarized below from this reference.

163. The orthographic map projection takes a selected projection point on the earth's surface, at latitude θ_0 and longitude φ_0, and essentially flattens out the surface of the sphere around that point. A viewing direction vector, (v_x,v_y,v_z), defines the direction in which the viewer is looking when viewing the earth, which is the negative of the vector

from the centre of the earth to the projection point. With R representing the (mean) radius of the earth, or about 3437.8 nautical miles:

$$(v_x, v_y, v_z) = (-R\cos\theta_0 \cos\phi_0, -R\cos\theta_0 \sin\phi_0, -R\sin\theta_0) \quad \text{(A1)}$$

164. The projection matrix, *M*, has the following entries:

$$\begin{aligned}
&M(1,1) = v_y / D_2 \\
&M(1,2) = -v_x / D_2 \\
&M(1,3) = 0 \\
&M(2,1) = -v_x v_z /(D_2 D_3) \\
&M(2,2) = -v_y v_z /(D_2 D_3) \\
&M(2,3) = D_2 / D_3 \\
&where\ D_2 = \sqrt{v_x^2 + v_y^2} \\
&and\ D_3 = \sqrt{v_x^2 + v_y^2 + v_z^2}
\end{aligned} \quad \text{(A2)}$$

165. This matrix will project any point on the surface of the earth to a two-dimensional map. The projection point itself is mapped to the origin of this Cartesian coordinate system. Any other point on the earth's surface at latitude θ (northern latitudes are positive) and longitude φ (western longitudes are negative) will have projected coordinates (*X*,*Y*) given by the matrix product of *M* with the coordinate vector of that earth point.

$$\begin{aligned}
&(x, y, z) = (R\cos\theta\cos\phi, R\cos\theta\sin\phi, R\sin\theta) \\
&(X, Y) = M \cdot (x, y, z)
\end{aligned} \quad \text{(A3)}$$

Annex B
Calculating a Random Normal Deviate

166. Abramowitz and Stegun [11], pages 952-3, offer a number of ways to calculate a random Normal deviate using a Uniform random number generator on the interval [0,1]. These include fitting a polynomial to the inverse cumulative Normal distribution, simply adding a large number of Uniform random numbers, a ‘Direct Method’ (see below), or using an Acceptance-Rejection method with a simpler function.

167. The contractor is free to choose any method, but the ‘Direct Method’ of the reference is recommended. It is described as follows. Given two Uniform random numbers from the interval [0,1], U1 and U2, the following will be a random Normal deviate with mean 0 and standard deviation 1.

$$x = \sqrt{-2\ln(U_1)}\ \cos(2\pi U_2) \qquad \text{(B1)}$$

This page intentionally left blank.

Annex C
Calculating the 'Radius of Positional Uncertainty' (RPU) For New Target Acquisitions

168. When a sensor detects a surface ship target and the resulting information is passed to the data fusion centre, there will be some degree of uncertainty about the location of the target when that information is used in updating the Recognized Maritime Picture (RMP). This will be represented as the Radius of Positional Uncertainty (RPU), as defined below. RPU is a central construct of the S6 model.

Probabilistic Representation

169. A general Bivariate Normal distribution is commonly employed to describe positional accuracy in two dimensions probabilistically. It suits passive cross-fixing systems such as High Frequency Direction Finding (HFDF) or passive sonar. Generally three parameters are required to define this distribution about a given position: the orientation of the major axis and the standard deviations in both the major and minor axes.

170. However, the simplified version of the Bivariate Normal, the Circular Normal, is an attractive choice of probability distribution for modelling. It requires only a single parameter to define it about a given position - the standard deviation, σ, in either orthogonal direction - and is much easier to work with. The Circular Normal is assumed to be a reasonable distribution for target location errors associated with most sensors that would operate from land, sea, air, or space. This is acknowledged to be perhaps a poorer assumption for the passive cross-fixing sensor systems mentioned above, but is adopted for practical reasons.

171. The Circular Normal is also known as the Rayleigh Distribution when it is transformed to have a single independent variable – range. These two distributions are discussed in detail by Emond [7]. The cumulative Rayleigh distribution gives the probability of the target being within a radius *r* from the reference point, and is given by Emond as:

$$P(r) = 1 - e^{-r^2 / 2\sigma^2} \qquad \text{(C1)}$$

172. Input system accuracies are often available as a Circular Error Probable (CEP), defined as the radius of a circle that has a 50 percent chance of including the target. Plugging P = 0.5 into (C1) yields the conversion factor to determine the required Circular Normal parameter σ

$$\sigma = 0.8493\ CEP \qquad \text{(C2)}$$

173. The radius of a circle, $r(P)$, achieving any given cumulative probability, P, of including the actual position of the target can be solved from (C1) in terms of a multiplicative factor on σ.

$$r(P) = \sqrt{-2\ \ln(1-P)}\ \sigma \qquad \text{(C3)}$$

174. For example:

$$r(0.95) = 2.4477\ \sigma$$
$$r(0.99) = 3.0349\ \sigma$$
$$r(0.995) = 3.2552\ \sigma$$

Definition: Radius of Positional Uncertainty (RPU_P)

175. The RPU is nominally defined in this Circular Normal context. It is the smallest radius around the detected coordinates of the datum that is has a user-defined chance, *P*, of including the target. A value of $P = 0.99$ might be a common choice, but the user can select this value.

176. The two main factors that determine the size of this uncertainty radius are:

a. The inherent **accuracy** of the sensor system in locating the target; and

b. The **latency** experienced in getting the information into the data fusion (RMP updating) process, considering that the target has likely moved during that time period.

Accuracy

177. Given the input value of Circular Error Probable (CEP) for sensor accuracy, the standard deviation parameter associated with this component of error, σ_A, is given by equation (C2) above.

$$\sigma_A = 0.8493\ CEP \qquad (C4)$$

Latency

178. Modelling the latency aspect of uncertainty is more challenging, as we have to develop an understanding of - and ultimately some probabilistic representation of - the behaviour of ships in that gap of time during which we weren't monitoring them. We know how much time has passed since the target was last detected. We know roughly how fast a surface ship of its class (if class is known) could have travelled during that time. We also might have some indication of the target's last known velocity vector, and of the assumed propensity of ships of its class (again, if known) to have stayed on the course that it was last seen travelling.

179. Devising a probability model to describe the location of the target after an elapsed time *T* travelling from a known starting point would be a severe challenge and would require numerous assumptions that would be difficult at best to validate. It has been decided to take a heuristic approach in combining these latency factors within the context of the Circular Normal model for positional uncertainty, as follows.

Latency Option 1 – Target Has No Propensity to Follow Initial Course.

180. The formulas in this subsection will apply if

a. The sensor was unable to establish a velocity vector (Note: the process of updating the RMP can enable a velocity vector to be estimated by differencing the last known position with the current, but this type of velocity estimate is discussed under Annex D, Propagating Positional Uncertainty Over Time); or

b. The ship class is unknown; or

c. The particular class of ship is known but that class has been assigned zero propensity to follow its last known course, as indicated by an assigned Heading Consistency Factor (HCF) value of 0 (Note: HCF = 0 might be applicable to fishing vessels that simply move around in seemingly random fashion within a fishing zone.)

181. Assume T_L is the information latency time. Assume V_P is the speed limit for that class of ship (if known, or an assumed general value for all ships if not known) at the *P* probability level. That is, the ship would travel no greater than this speed *P* percent of the time. Maximum speeds of ships are generally well known, so this parameter should be easy to estimate. The physical limits of ship propulsion will likely result in $V_{0.95}$, $V_{0.99}$, or $V_{0.999}$ all being pretty much within a knot of each other.

182. The product of these two variables, $T_L V_P$, represents the maximum radius about the last known position that is guaranteed to have no worse than a *P* percent chance of including the target. This represents the worst-case scenario where the target pursues an unknown straight-line course during the entire time interval T_L. In lieu of making any other assumptions about the motion of the ship while we weren't monitoring it, we will simply make the conservative assumption and permit this radius to represent the probability level *P* in the Circular Normal distribution.

183. Therefore, the Circular Normal standard deviation equivalent for latency, σ_L, is calculated from (C3):

$$\sigma_L = \frac{T_L V_P}{\sqrt{-2\ln(1-P)}} \tag{C5}$$

184. We can now take advantage of the Addition Theorem for Normally distributed random variables: the sum of two random Normal deviates is itself Normally distributed with variance equal to the sum of the individual variances. This yields a combined Accuracy and Latency error as

$$\sigma = \sqrt{\sigma_A^2 + \sigma_L^2} \tag{C6}$$

185. The final Radius of Positional Uncertainty is calculated as

$$RPU_P = \sqrt{-2\ln(1-P)}\ \sigma \tag{C7}$$

186. This radius, applied around the target's detected location, defines a circle that will include the actual position of the target with probability *P*.

Latency Option 2 – Target Has Propensity to Follow Initial Course

187. This portion of the algorithm will only be followed when the following conditions apply:

a. The Sensor was able to estimate the target's velocity vector; and

b. The Sensor was able to determine the target's classification; and

c. The Ship Class is assigned a Heading Consistency Factor (HCF) value that is non-zero

188. The algorithm will apply a third type of error, σ_{DR} in this case to account for uncertainty in the dead reckoning of the ship's position at time T_L later. It will also apply the final three-factor RPU estimate about a different point – one that is somewhere between the original detected position and the target's dead-reckoned position at time T_L.

189. Let *V* be the target's assessed speed, σ_V be the standard deviation of the Sensor's error in estimating target speed (a basic input), *H* be the target's assessed heading (degrees from true north), and σ_H be the standard deviation of the Sensor's error in estimating target heading (in degrees, a basic input as well). Both *V* and *H* can be reasonably assumed to be Normally distributed. If the target maintained the same speed and heading over the latency period, then the standard deviations in range and deflection dimensions can be suitably scaled. They are unlikely to be identical, so to convert to our Circular Normal model an average standard deviation will be calculated

$$\sigma_{DR} = \frac{T_L \sigma_V + V\ T_L \sigma_H (\pi / 180)}{2} \qquad \text{(C8)}$$

190. Note that we average the standard deviations here, not the variances, as we are not summing two errors. The three errors represented by the standard deviations σ_A, σ_L, and σ_{DR} are now combined in a heuristic algorithm that brings in the Heading Consistency Factor, HCF. This is presented in equation (C9).

$$\sigma = \sqrt{\sigma_A^2 + (1 - HCF)\ \sigma_L^2 + HCF\ \sigma_{DR}^2} \qquad \text{(C9)}$$

191. The final standard deviation will always include the accuracy term, as that is a fundamental source of positional error regardless of what assumptions of future target mobility are made. If HCF was assigned a value of 0 then equation (C6) applies, effectively 'weighting' the latency error fully (a value of 1) and the irrelevant dead reckoning error not at all (a value of 0). At the other extreme, if HCF was assigned a value of 1 we would be assured that the target would be following its determined course and velocity over the latency interval. In this case, the latency term is irrelevant (with a weight of 0) and the dead reckoning term fully relevant (with a weight of 1). Therefore, weighting the variances according to the HCF value assigned would appear to be a reasonable heuristic.

192. The final RPU value is calculated as per equation (C7) using this value of σ.

193. The only remaining question relates to what geographic position this RPU value should be centred upon. Again, with HCF = 0 we would be reverting to the Option 1 situation where the RPU is centred on the last known position of the target, denoted (x_0,y_0). With HCF = 1 the RPU would be centred on the dead reckoned position, (x_{DR},y_{DR}). So, again, centring the RPU at a position linearly interpolated between the last known position and dead reckoned position according to the HCF value assigned would appear to be a reasonable heuristic.

$$\begin{aligned}(x_{DR}, y_{DR}) &= (x_0 + V\sin(H), y_0 + V\cos(H)) \\ (x_{RPU}, y_{RPU}) &= (1 - HCF)(x_0, y_0) + HCF\,(x_{DR}, y_{DR})\end{aligned} \qquad \text{(C10)}$$

Summary

194. The mathematical method espoused in this Annex is also applied in Annex D when the growth of positional uncertainty over time for Tracked Targets (TT) is discussed. The RPU_P value is calculated as primarily a radius to be used for display purposes. The underlying Circular Normal standard deviation parameter, σ, will always be the working variable for calculations, and as discussed in the Data Fusion chapter (Chapter 5), a circle of larger radius representing the square root of P will be used when determining if a new sensor datum (SD) and a current TT in the RMP are compatible.

195. The use of the Heading Consistency Factor permits TT to be predictive in where they will appear in the future. This is effectively a discrete implementation of a Kalman filter.

This page intentionally left blank.

Annex D
Propagating Positional Uncertainty Between RMP Updates

196. Once a Tracked Target (TT) has been established within the Recognized Maritime Picture (RMP), it will continue to exist over time until it is either updated or discarded. The Data Fusion algorithm will check every datum within a new Sensor Data (SD) overlay to see if it potentially matches a given TT in the RMP. Our uncertainty in knowing the target's precise location will have expanded, as the target may have moved considerably during the interval since it was last updated. This growth in positional uncertainty is modelled in the same fashion as the 'latency' factor associated with new detections, as outlined in Annex C.

197. Let T_I represent the time interval between the previous update of the TT and the current time. At the time of previous update, a total Radius of Positional Uncertainty (at the P probability level), U, would have been calculated. The Circular Normal standard deviation parameter, σ_U, is related to the RPU_P value by rewriting (C7) as:

$$\sigma_U = \frac{U}{\sqrt{-2\ \ln(1-P)}} \tag{D1}$$

198. The TT may or may not have a velocity vector currently assigned to it. If it does, the speed value and the heading value both will have standard deviations of error associated with them, σ_V (in knots) and σ_H (in degrees), respectively. If the last update datum provided an accurate velocity vector estimate then these values, including the error standard deviations associated with that sensor, are inherited by the TT. If the last update did not provide that data but there was at least one previous update for this TT, then the velocity vector will be estimated by the time-differenced position over time values for those two updates. Global values for the speed and heading error standard deviations will be employed in this case. See Annex L for details on the velocity vector updating process. The remaining possibility is that the TT has never been updated and the initial acquisition datum was from a sensor without velocity estimation capability. In this case, no velocity vector is associated with the TT.

Positional Uncertainty Propagation Option 1: Tracked Target has no propensity to follow its initial course

199. The formulas in this subsection will apply if

a. There is no velocity vector associated with the TT; or

b. The ship class is unknown; or

c. The particular class of ship is known but that class has been assigned zero propensity to follow its last known course, as indicated by an assigned Heading Consistency Factor (HCF) value of 0.

200. As per Annex C, we assume V_P is the speed limit for that class of ship (if known, or an assumed generic value for all ships if not known) at the user-defined *P* probability

level. That is, the ship would travel no greater than this speed P percent of the time. The product $T_I V_P$ represents the maximum radius about the last known position that is guaranteed to have no worse than a P percent chance of including the target. As discussed in Annex C, this represents the worst-case scenario where the target pursues an unknown straight-line course during the entire time interval. We make this conservative assumption and permit this radius to represent the probability level P in the Circular Normal distribution.

201. Therefore, the Circular Normal standard deviation equivalent for possible travel during the update interval, σ_I, is calculated as:

$$\sigma_I = \frac{T_I V_P}{\sqrt{-2\ln(1-P)}} \tag{D2}$$

202. Again, taking advantage of the Addition Theorem for Normally distributed random variables, we can reasonably represent the combined positional error as Circular Normal with variance equal to the sum of the individual variances. This yields a combined positional error at the current time of

$$\sigma = \sqrt{\sigma_U^2 + \sigma_I^2} \tag{D3}$$

203. This error is applied around the position of the previous update.

Positional Uncertainty Propagation Option 2: Tracked Target has propensity to follow its initial course

204. This portion of the algorithm will only be followed when the following conditions apply:

a. The TT has a velocity vector estimate; and

b. The classification of the TT is known; and

c. The TT's Ship Class has been assigned a HCF value that is non-zero.

205. In the same fashion as Annex C, the error propagation algorithm will also consider the dead reckoning error and apply it in proportion to the HCF value assigned to the known ship class. And the algorithm will apply the final Circular error estimate about a different point – one that is between the previous update location and the target's current dead-reckoned position, as weighted by the HCF value.

206. Let V be the TT's assigned speed at the previous update, σ_V be the assigned standard deviation in that speed estimate, H be the TT's assigned heading at the previous update, and σ_H be the standard deviation in that estimate (both in degrees). Both V and H are reasonably assumed to be Normally distributed. If the TT maintained the same speed and heading since its last update, then the standard deviations in range and deflection dimensions can be suitably scaled. They are unlikely to be identical, so to convert to our Circular Normal model an average standard deviation will be calculated

$$\sigma_{DR} = \frac{T_I \sigma_V + V\, T_I \sigma_H \left(\pi / 180\right)}{2} \qquad \text{(D4)}$$

207. The three errors represented by the standard deviations σ_U, σ_I, and σ_{DR} are now combined in a heuristic algorithm that brings in the Heading Consistency Factor, HCF. This presented in equation (D5).

$$\sigma = \sqrt{\sigma_A^2 + (1 - HCF)\, \sigma_L^2 + HCF\ \sigma_{DR}^2} \qquad \text{(D5)}$$

208. The final standard deviation will always include the original error term at the time of the previous update, represented by σ_U. If HCF was assigned a value of 0 then equation (D3) applies, effectively 'weighting' the time interval error fully (a value of 1) and the irrelevant dead reckoning error not at all (a value of 0). At the other extreme, if HCF was assigned a value of 1 we would be assured that the TT had been following its established course and velocity over the update interval. In this case, the time interval term is irrelevant (with a weight of 0) and the dead reckoning term fully relevant (with a weight of 1). Therefore, weighting the variances according to the HCF value assigned would appear to be a reasonable heuristic.

209. What geographic position should this error value be centred upon? Again, with HCF = 0 we would be reverting to the Option 1 situation where the error is centred on the position of the TT from its last update, denoted (x_U, y_U). With HCF = 1 the error would be centred on the dead reckoned position, (x_{DR}, y_{DR}). So, again, centring the error at a position, (x,y), linearly interpolated between the last updated position and the current dead reckoned position according to the HCF value assigned would appear to be a reasonable heuristic.

$$\begin{aligned} (x_{DR}, y_{DR}) &= (x_U + V \sin H, y_U + V \cos H) \\ (x, y) &= (1 - HCF)(x_U, y_U) + HCF\,(x_{DR}, y_{DR}) \end{aligned} \qquad \text{(D6)}$$

Summary

210. When the possibility of a new update for the TT is being checked with a new SD overlay, the value of σ calculated by the appropriate formula above - (D3) or (D5) - will be converted to an appropriate RPU circle about the position established in (D6) and entered into the Data Fusion calculation.

211. As discussed in more detail in the Data Fusion algorithm section, the circles will be extended beyond the P probability level radius to √P. The intersection region of two circles (one representing the TT and the other representing the new SD datum), each of which have a √P chance of including the actual target will yield a (√P)(√P) = P chance of including the target.

$$RPU_{\sqrt{P}} = \sqrt{-2 \ln(1 - \sqrt{P})}\ \sigma \qquad \text{(D7)}$$

This page intentionally left blank.

Annex E
Computing the Intersection of Two Circles

212. The area of intersection of two circles, *A*, is easily derived from basic principles. Assume there are two circles of radius *R* and *r*, where $R \geq r$. A distance *D* separates the centres of the circles. Figure E-1 depicts the four cases of circle separation to consider.

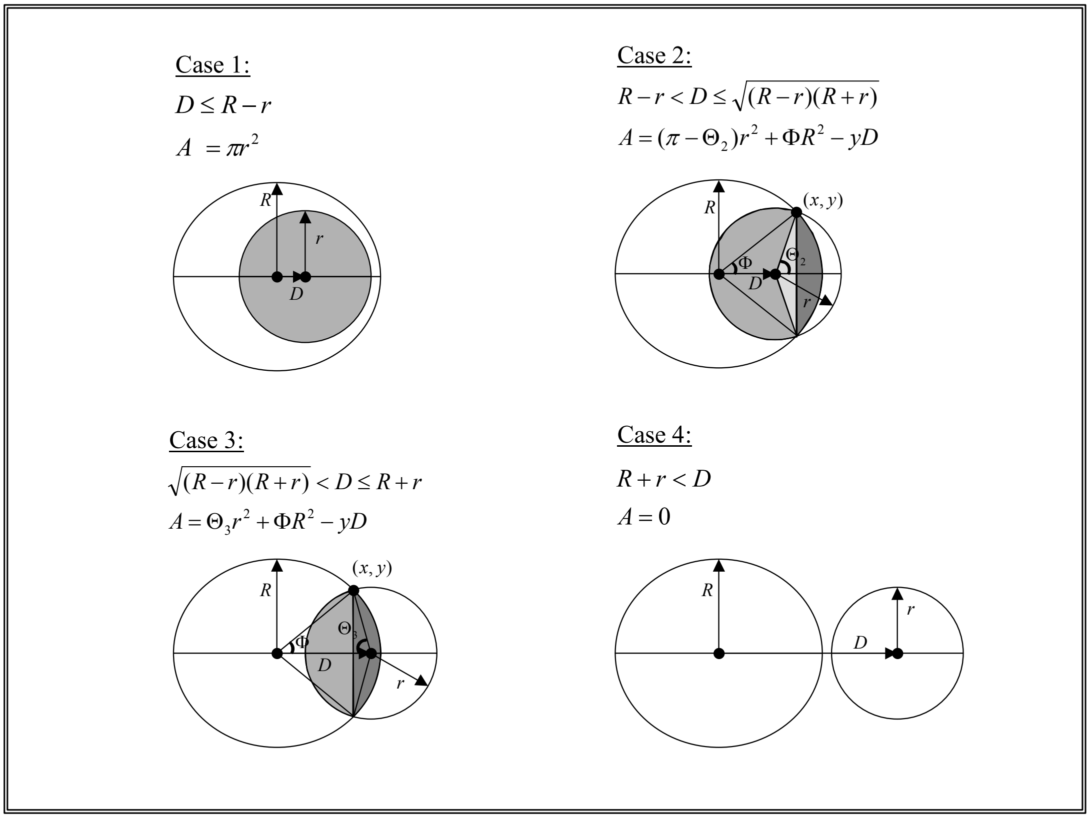

Figure E-1. *Four Cases of Circle Intersection*

Case 1: $D \leq R - r$

213. In this situation the smaller circle is completely contained within the larger circle.

$$A = \pi r^2 \tag{E1}$$

Case 2: $R - r < D \leq \sqrt{(R-r)(R+r)}$

214. Now the smaller circle is just beginning to emerge from the larger circle. The two circles intersect. Considering the centre of the larger circle to be the origin of the plane, the intersection points, (x,±y), can be calculated as follows:

$$x = \frac{D^2 + R^2 - r^2}{2D}$$
$$y = \pm\sqrt{\frac{(2D-1)R^2 - D^2 + 1}{2D}} \qquad \text{(E2)}$$

215. The half-angles subtended at the centre of both circles by the intersection points are (all angles in radians)

$$\theta_2 = \cos^{-1}\left(\frac{x-D}{r}\right)$$
$$\phi = \cos^{-1}\left(\frac{x}{R}\right) \qquad \text{(E3)}$$

216. Total area of intersection can be broken into the three sections shaded in grey in Figure E-1. The first section, the left-most shaded area in the figure, is a majority-sized sector of the small circle, reduced from the total area of the circle as defined by θ_2:

$$A_1 = \frac{2\pi - 2\theta_2}{2\pi}\pi r^2 = (\pi - \theta_2)r^2 \qquad \text{(E4)}$$

217. The second (middle shaded) section is triangular. Half the base times the height gives:

$$A_2 = \frac{2y(x-d)}{2} = y(x-D) \qquad \text{(E5)}$$

218. The third (right shaded) section is a lens-shaped piece of the larger circle. This is the area remaining when the sector defined by φ on both sides of the x-axis is reduced by the area of the triangle between the same three points. Using the same arguments as above, this is

$$A_3 = \phi R^2 - xy \qquad \text{(E6)}$$

219. The final area is the sum of these three sub-areas:

$$A = A_1 + A_2 + A_3$$
$$A = (\pi - \theta_2)r^2 + \phi R^2 - yD \qquad \text{(E7)}$$

Case 3: $\sqrt{(R-r)(R+r)} < D \leq R + r$

220. Now the smaller circle has moved very much outside the larger circle. The area of intersection is the sum of the two shaded lens-shaped regions, as depicted in Figure E-1.

Employing the same definitions above for *x*, *y*, and φ, we will redefine the angle within the smaller circle (just to keep all quantities positive) as

$$\theta_3 = \cos^{-1}\left(\frac{D-x}{r}\right) \tag{E8}$$

221. The first (left-most in the Figure) 'lens' is the sector of the smaller circle defined by twice the half-angle θ_3, less the triangle subtended by the same three points: $(x,\pm y)$ and the centre of the smaller circle.

$$A_1 = \theta_3 r^2 - (D-x)y \tag{E9}$$

222. The second lens is the sector of the larger circle defined by twice the half-angle φ, less the corresponding triangle in that circle.

$$A_2 = \phi r^2 - xy \tag{E10}$$

223. The intersection area is the sum of these two lenses

$$\begin{aligned} A &= A_1 + A_2 \\ A &= \theta_3 r^2 + \phi R^2 - yD \end{aligned} \tag{E11}$$

Case 4: $R + r < D$

224. This is the trivial case where the circles are so far apart they do not intersect.

$$A = 0 \tag{E12}$$

Modelling the Intersection Region

225. Once the Data Fusion algorithm has matched a Sensor Datum to an existing Tracked Target, it will assign the intersection area as the updated zone of positional uncertainty at the assigned level of probability, P. In order to continue propagating the Circular Normal model, the intersection area will be converted into a circle about a point. The area of the circle will be the intersection area calculated above, which will be assumed to represent the Radius of Positional Uncertainty at the P probability level, RPU_P. The standard deviation parameter of the Circular Normal distribution for the updated TT location can be calculated as in Annex D:

$$\begin{aligned} RPU_P &= \sqrt{A/\pi} \\ \sigma &= \frac{RPU_P}{\sqrt{-2\ln(1-P)}} \end{aligned} \tag{E13}$$

226. The position of the TT will have to be updated as well. The exact centroid of the intersection region could be calculated exactly with a complicated integral if desired. But

since we are making the coarse conversion of a "squashed football"-shaped region into a circle anyway, then the centroid calculation does not need to be excessively precise.

227. The intersection will be bounded between the left edge in Figure E-1 at $x = D\text{-}r$ and the right edge at $x = R$. Splitting this difference defines a reasonable centre point for a circle of the same area as the intersection area.

228. Therefore, if we let (x_R,y_R) and (x_r,y_r) represent the centres of the two circles of radius R and r, respectively, in two dimensional space, then the coordinates of the centre of the updated circle, (x_C,y_C), would be

$$\begin{aligned} &D = \sqrt{(x_R - x_r)^2 + (y_R - y_r)^2} \\ &W_R = (D - R + r)/2D \qquad (0 \le W_R \le 1) \\ &W_r = (D - r + R)/2D \qquad (0 \le W_r \le 1) \\ &(x_C, y_C) = W_R(x_R, y_R) + W_r(x_r, y_r) \end{aligned} \tag{E14}$$

229. These equations hold for the main two Cases, 2 and 3 above, where $R\text{-}r < D \le R+r$. However, if we adopt the rule that the weights W_R and W_r are truncated to 0 if equation (E14) calculates a negative value, or truncated to 1 if (E14) calculates a value greater than 1, then this formulation will hold for all the non-trivial cases ($D \le R+r$).

230. If $D = 0$ then clearly either circle centre can be used.

Annex F
Scheduling the Next Event in a Poisson Process

231. A Poisson Process with a mean of λ occurrences per unit time will have a distribution of inter-arrival times that is exponentially distributed (see Parzen [12], Theorem 3A, Pg 135) as:

$$f(t) = \lambda e^{-\lambda t} \qquad \text{(F1)}$$

232. The cumulative exponential is

$$F(T) = \int_0^T f(t)\,dt = 1 - e^{-\lambda T} \qquad \text{(F2)}$$

233. If a uniform random number *R* on the interval [0,1) is drawn, then a random exponential time deviate can be derived by solving (F2) for T.

$$T = -\frac{\ln(1-R)}{\lambda} \qquad \text{(F3)}$$

Randomizing Hardware Failures

234. Given the Mean Time Between Failures (*MTBF*) and a time interval *T*, the probability of the system failing in that time interval is given by (F2), where $\lambda = 1/MTBF$.

235. A uniform random number on the interval [0,1] can be drawn and compared to this probability. If it is less than that value, the system will be deemed to have failed during that interval.

236. Given a Mean Time To Repair (*MTTR*), a random exponential time deviate can be derived from a uniform random number *R* via (F3) above, where $\lambda = 1/MTTR$. This time determines when the system will be functioning again.

This page intentionally left blank.

Annex G
Operations With Convex Polygons

Determining if a Polygon is Convex

237. Assume a sequence of vertices, $V_1 = (x_1,y_1)$, $V_2 = (x_2,y_2)$, …,$V_n = (x_n,y_n)$, forms a polygon in two dimensions (V_n is rejoined to point V_1 to complete the polygon).

238. A cross-product algorithm for determining if this polygon is convex can be derived from basic principles. The algorithm is based on the fundamental principle that, as one progresses around a convex polygon, the next edge must always be turning in the same direction, always right or always left (or it could be through a redundant vertex where the next edge is heading in exactly the same direction). The proof is left to the reader.

239. Calculate the sign, S_i, of the z-component (into or out of the two-dimensional plane) of the cross-product of the vectors through each point V_i.

$$S_i = Sign[(x_{i+1} - x_i)(y_i - y_{i-1}) - (x_i - x_{i-1})(y_{i+1} - y_i)] \qquad \text{(G1)}$$

240. Of course, the n+1st point is 1, and the 0th point is n. The sign function returns +1 if the calculation is positive, 0 if the calculation is 0, and –1 if the calculation is negative.

241. If the product of any pair of S_i equals –1 then the polygon is not convex.

Determining if a Point Lies Within a Convex Polygon – Algorithm A

242. Given an arbitrary point $W = (x,y)$ on the plane, this same method can be employed to determine whether or not that point lies within the defined (convex) polygon.

243. The fundamental principle is that, as one fans around point W looking at each of the V_i in sequence, the direction of turn to the next vertex is always the same – always to the right or always to the left (although it could remain stationary occasionally). Again, the proof is left to the reader.

244. Calculate the sign, S_i, of the z-component of the sequential cross-product of the vectors emanating from W to each polygon vertex point V_i.

$$S_i = Sign[(x_{i+1} - x)(y_i - y) - (x_i - x)(y_{i+1} - y)] \qquad \text{(G2)}$$

245. Again, the n+1st point is 1. And like before, if the product of any pair of S_i is –1 then the point must be exterior to the polygon.

Determining if a Point Lies Within a Convex Polygon – Algorithm B

246. There are other algorithms that the contractor may wish to employ to optimize performance. One is to pre-calculate the equations of the infinite lines forming the edges of the polygon when the convexity checking is being done, which are then stored in a

matrix. The product of the matrix with the position vector yields a vector that simply has to be sign checked to ensure the point in question is properly above or below each line. MATLAB employs this type of routine. The tradeoff is between execution speed and storage. Thanks to Rick McCourt for compiling the following description of this class of algorithm.

247. The convex polygon defined by the vertices V_i can be represented in matrix form,

$$\mathbf{Ax} = \mathbf{b}, \tag{G3}$$

where

$$\mathbf{A} \in R^{n\,x\,2}$$
$$\mathbf{b} \in R^{n\,x\,1}$$
$$\mathbf{x} = \begin{bmatrix} x & y \end{bmatrix}^T$$

248. Each row in (G3) represents one side of the convex polygon. If the i^{th} side is horizontal, i.e. $y_i - y_{i+1} = 0$, then the i^{th} row is,

$$\begin{bmatrix} 0 & 1 \end{bmatrix}\begin{bmatrix} x \\ y \end{bmatrix} = b_i$$

and if the i^{th} side is vertical, i.e. $x_i - x_{i+1} = 0$, then the i^{th} row is

$$\begin{bmatrix} 1 & 0 \end{bmatrix}\begin{bmatrix} x \\ y \end{bmatrix} = b_i$$

249. If the i^{th} side does not fall into either of the above descriptions, then the equation for the i^{th} side is $y = m_i x + b_i$. Using the vertices V_i and V_{i+1} the values of m_i and b_i can be determined:

$$m_i = \frac{y_i - y_{i+1}}{x_i - x_{i+1}},$$

$$b_i = \frac{y_{i+1}x_i - y_i x_{i+1}}{x_i - x_{i+1}}.$$

250. Of course, the n+1st point is the 1st. Now the i^{th} row of (G3) can be formed using these values,

$$\begin{bmatrix} -m_i & 1 \end{bmatrix}\begin{bmatrix} x \\ y \end{bmatrix} = b_i$$

251. To ensure that the inequality, $\mathbf{Ax} \le \mathbf{b}$, represents the interior of the convex polygon, certain rows may need to be multiplied by -1. To check this, choose any vertex not used in the description of the i^{th} side and test if,

$$\boldsymbol{A_i}\ \boldsymbol{x_j} \le b_i \tag{G4}$$

where $\boldsymbol{A_i}$ is the i^{th} row of **A**, b_i is the i^{th} row of **b**, and $\boldsymbol{x_j}$ is the chosen test vertex. If the evaluation of (G4) is false, multiply all elements in the row by -1 and continue with the next side of the polygon.

252. In the end, if a given point, $\boldsymbol{x} = [x \;\; y]^T$, on the plane satisfies the matrix inequality, $Ax \le \mathbf{b}$, then that point lies within the defined convex polygon.

Calculating the Area of a Convex Polygon

253. The area of a convex polygon is easily derivable from basic principles as well.

254. For any edge, (x_i,y_i) to (x_{i+1},y_{i+1}), the area between that edge and the x-axis is simply the difference in x times the average value of y. The calculated value may be a positive or negative area, but if the vertex pairs are taken in order around the perimeter of the polygon, the sum of the areas calculated this way will give a net addition whose absolute value correctly gives the polygon's area. The proof is left to the reader, but the following formula delivers the area of a polygon. Since this is a closed polygon, point n+1 is identically point 1.

$$Area = \left| \sum_{i=1}^{n} (x_i y_{i+1} - x_{i+1} y_i) \right| \qquad \text{(G5)}$$

Randomly selecting a point within a defined region

255. Two methods are provided for doing this is. Method 1 has the desirable property of uniformity. That is, any point in the region has equal probability of being selected. It works for a convex polygon or a complex region defined by a set of convex polygons. However, it is only applicable for selecting points within a region that has a non-zero area (i.e. is not a line). Method 2 is computationally more direct and is required if the region has no area (i.e. it is a line). However, it only works for a single convex polygon, not on sets of polygons. It has not been proven to have the uniformity property.

256. Both methods will be implemented and the simulation will determine which one to apply in the situation. The user may be given the option to choose which method to apply in the case of a single convex polygon.

257. **Method 1** (areas only). Determine the minimum and maximum values of x and y from the coordinates of all the vertices for all of the convex polygons in the set (the set can be a single polygon). Then select two random numbers, x_0 and y_0, uniformly from the intervals $[x_{min}, x_{max}]$ and $[y_{min}, y_{max}]$, respectively. If the point (x_0, y_0) lies inside one of the convex polygons, as determined using the process above and (G2), then accept it. Otherwise, draw a new pair of random numbers.

258. **Method 2** (lines or single convex polygonal areas). Draw a uniformly distributed random number on the interval [0,1] for each vertex point of the convex region. Normalize these numbers so they sum to 1, yielding weights w_i for each vertex. Then compute the weighted sum of the vertex coordinates, using this point as the selection:

$$(x, y) = \left(\sum_i w_i x_i , \sum_i w_i y_i \right) \tag{G6}$$

Annex H
Determining the Horizon for Conventional Radars

259. Conventional ground-based radars operate in frequency bands that demand a direct path between the radar and the target ship. Radar waves will bend slightly through the atmosphere, behaving as if the earth had a radius that was 4/3 times its actual value. This common "four-thirds earth" rule (see Skolnik [8], page 496) gives the following formula for determining the distance to the radar horizon

$$H = 1.228\,(\sqrt{h_R} + \sqrt{h_T}) \qquad \text{(H1)}$$

where h_R is the height of the radar above sea level and h_T is the height of the target above sea level. Both values are given in **feet**, yielding a value of H in **nautical miles**.

This page intentionally left blank.

Annex I
Modelling Maximum Detection Range for Surface Wave Radar

260. The maximum range depends on the day, the time of day (daytime or night time), the class of ship, and the aspect that ship presents to the SWR.

261. If the bearing from the SWR to the ship is *B* degrees and the heading of the ship is *H* degrees, then the aspect presented to the radar is *B-H* degrees. We will assume that the square of the sine and cosine of this angle are reasonable representations of the weights to assign to the beam and bow/stern aspects. Letting D_{Bm} and $D_{B/S}$ represent the respective average maximum daytime detection ranges (beam and bow/stern aspect) for SWR against the given class of ship, then the average maximum daytime detection range accounting for aspect, D_A is:

$$D_A = \sin^2(B - H)D_{Bm} + \cos^2(B - H)D_{B/S} \qquad \text{(I1)}$$

262. On any given day, the nature of ionospheric clutter will vary, which has a big influence on maximum detection range. At the first SWR update in a given day (Day 1 begins at time 0, Day 2 at time 24.00, etc.), a random maximum range adjustment value, Δ, is determined by drawing a random Normal deviate against the specified standard deviation (see Annex B). This value is carried throughout the day.

263. Performance of SWR has diurnal variability as well. The user specifies the daytime hour range as global parameters. If it is determined that it is nighttime, then a multiplicative factor, F_N, is applied to the maximum range value. The final maximum range is

$$R_{Max} = (D_A + \Delta)\, F_N \qquad \text{(I2)}$$

This page intentionally left blank.

Annex J
Modelling Satellite Coverage

264. We are given the orbital inclination of the surveillance satellite, I, the orbital period, T, the central latitude of the Regional View, L, and the swath width of the sensor, S. Angles are in degrees, time in hours, and distance in nautical miles.

265. The orbital inclination is the angle that the satellite ground track makes with the equator as it passes overhead from south to north (i.e. is 'ascending'). This is identically the maximum latitude that the satellite will pass over.

Using the Sun-Synchronous Model

266. Many surveillance satellites like RADARSAT, SPOT, etc. operate in circular, sun-synchronous orbits. These are special near-polar orbits. The extra girth of the earth at the equator causes satellites in these orbits to precess at about 1 degree per day, which results in them maintaining the same position with respect to the sun as the year progresses. Sun-synchronous orbits typically will have an orbital inclination of about 98 degrees. The dawn-dusk orbit is particularly attractive for solar power generation as it results in the satellite never being in the earth's shadow.

267. A useful property of sun-synchronous orbits is that the points they pass over are always at the same local time (assuming continuous time zones) while ascending and 12 hours different while descending. Let us label these orbital time-of-day parameters H_A and H_D, respectively. This simple relationship between time of day and satellite longitude as the earth spins beneath it will enable our modelling approach to be simplified as well. We will tie time and longitude together. This will be accurate for sun-synchronous orbits, but will be missing a small correction factor for other angles of inclination.

268. The RADARSAT website [9] lists the orbital parameters for RADARSAT 1 and 2: circular orbit; orbital inclination 98.6 degrees; altitude 431 nm; period of 100.7 minutes (1.6783 hrs); ascending time of H_A = 1800 hours local, and descending time of H_D = 0600 hours local.

Projecting into the Cartesian Space

269. The satellite's sensor will sweep a path across the Regional View, which has been defined around the central latitude, L. A diagonal linear swath in the Cartesian space will quite reasonably approximate this. The angle of that diagonal is not quite the orbital inclination (unless L is zero degrees at the equator). The following formula, derived from basic principles, defines the adjusted angle, I_L, at which the satellite crosses latitude L.

$$I_L = \sin^{-1}\left(\sin I \sqrt{1 - \frac{\tan^2 L}{\tan^2 I}}\right) \qquad \text{(J1)}$$

270. Since I is always positive (between 0 and 180 degrees), equation (J1) will always produce a positive angle. Since the range of the inverse sine function is from -π/2 to π/2,

we must adjust when $I > \pi/2$ (90 degrees). In this case, I_L should be π *minus* the above angle. Note that this is identically I when L=0, is zero degrees when at maximum altitude (L=I) and is undefined for latitudes above this, of course. I_L is always shallower (closer to x-axis) than I.

271. Figure J1 depicts these constructs within the context of the Regional View with the satellite shown passing directly over the origin in an ascending direction. The RV is defined by its four corner points, ($\pm X_{Max}$,$\pm Y_{Max}$). There are three x-values, labelled A, B, and C in the Figure, that will combine to define the four corner points of the coverage zone, shown as a shaded parallelogram. The width of the parallelogram, when added to the RV width (equals 2 X_{Max}) defines an east-west window. If the satellite passes over the central latitude within that window then we know that it will be covering at least a corner of the RV.

272. In the S6 simulation, this window will be converted from a distance window to a time window. For every minute the ascending satellite crosses the central latitude before its ascending time value, the further east it will cross (and the opposite for later crossing times).

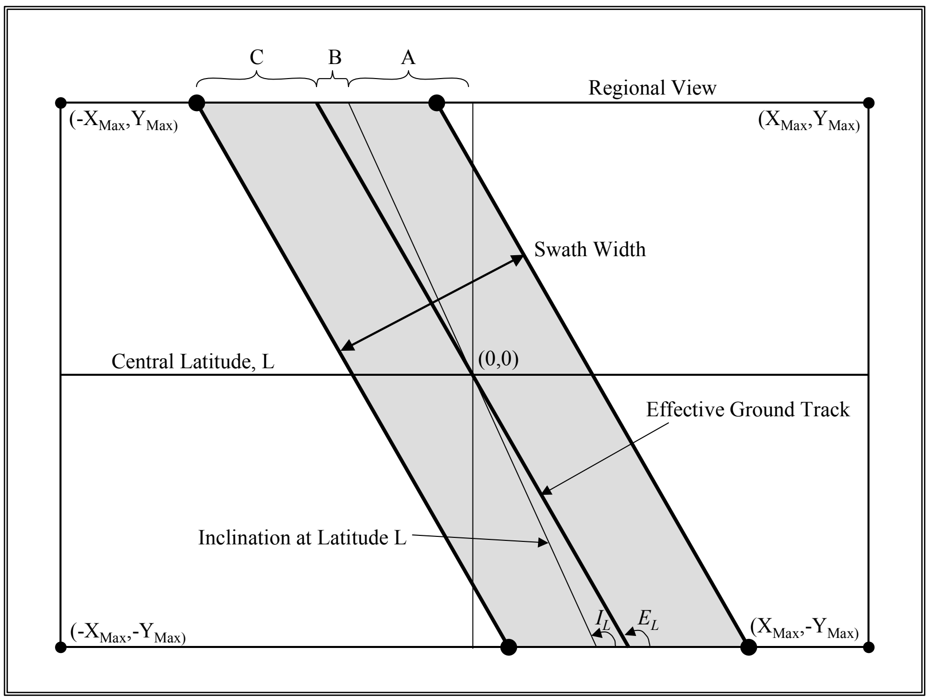

***Figure J-1**. Ascending Satellite Swath Through Regional View*

273. For calculation purposes, it is assumed that the swath covered by the surveillance satellite is centred on the satellite's ground path, but accuracy is not affected to any significant degree (at moderate latitudes in relation to the orbital inclination) if the swath is offset one side or the other from the ground track.

Calculating the Coordinates of the Parallelogram

274. The first *x*-value, *A*, is the satellite ground track offset at Y_{Max} induced by the orbital inclination at the central latitude as calculated by (J1), and will be negative or positive in value depending on I_L.

$$A = \frac{Y_{Max}}{\tan I_L} \tag{J2}$$

275. The second *x*-value, *B*, represents a correction required to account for the movement of the earth from west to east underneath the satellite as it traverses the Regional View. Dividing Y_{Max} by 60 (nm per degree of latitude) gives the approximate height in degrees of the latitude gap traversed between the central latitude and the time the satellite exits the north edge of the RV. Dividing by the cosine of the orbital inclination at the central latitude approximates the angle swept out by the satellite while traversing this latitude gap. The time it takes the satellite to cover this distance is approximately the fraction that angle represents of a total orbit of 360 degrees, times the orbital period. During this time, the earth is travelling west-to-east at a speed equal to the earth's circumference at that latitude divided by 24 hours. Hence, the distance *B* in Figure J-1 will be given by the following, where the mean radius of the earth, R_E, is about 3,438 nm:

$$B = velocity \cdot time = \frac{2\pi R_E \cos L}{24} \cdot \frac{(Y_{Max} /(60 \cos I_L)\, T}{360} \tag{J3}$$

276. *B* will always apply in a negative *x* direction at Y_{Max} and a positive *x* direction at -Y_{Max}. The combined value of *A* and *B*, denoted *D*, is now

$$D = \frac{Y_{Max}}{\tan I_L} - B \tag{J4}$$

277. Hence, the *effective* orbital inclination at latitude *L* accounting for earth rotation as the satellite passes over the RV, denoted E_L, is

$$E_L = \tan^{-1}\left(\frac{Y_{Max}}{D}\right) \tag{J5}$$

278. Since the earth spins from west to east under the satellite, this correction serves to further flatten the effective ground track over the RV if the orbital inclination value is over 90 degrees, as is the case with most sun-synchronous orbits. At lesser inclinations the rotation of the earth actually serves to make the effective swath inclination more upright.

279. The range of the inverse tangent function is from -π/2 to π/2. Hence, if (J5) produces a negative result (i.e. $E_L > \pi/2$ or 90 degrees), then E_L should be set to π *plus* the above negative angle.

280. The third *x*-value, *C*, accounts for the swath width:

$$C = \frac{S/2}{\sin E_L} \quad \text{(J6)}$$

281. Therefore, the four corners of the parallelogram in Figure J-1 are:

$$\begin{array}{l} (D - C, Y_{Max}) \\ (D + C, Y_{Max}) \\ (-D + C, -Y_{Max}) \\ (-D - C, -Y_{Max}) \end{array} \quad \text{(J7)}$$

282. If P_x is the largest x-value amongst the four corner points, then we can identify the east-west window ($-X_{Max}-P_x$, $X_{Max}+P_x$). If the satellite's ascending orbit crosses the central latitude within this window then the coverage parallelogram will overlap with some portion of the Regional View.

Shifting the Parallelogram East/West As Required

283. As mentioned earlier, the advantage of basing our modelling on sun-synchronous orbits is that we can use time windows to substitute for distance windows. If the satellite's orbital characteristic was an ascending time of H_A = 1800 hours, and the simulation projected the next time the satellite crossed the central latitude ascending was 1745 hours, then we know the satellite will be passing 15 minutes of earth rotation to the east of the origin of the Regional View at that time.

284. The time-to-distance conversion factor, F_{TD}, is the same velocity factor used in (J3).

$$\begin{aligned} F_{TD} &= \frac{2\pi R_E \cos L}{24} \\ \Delta H &= (X_{Max} + P_x)/F_{TD} \end{aligned} \quad \text{(J8)}$$

285. The equivalent time window now is $H_A \pm \Delta H$, where ΔH is as defined above. If the satellite's next ascending crossing time today at latitude L is within that time interval, then the coverage parallelogram overlaps the Regional View. Otherwise, we know it cannot intersect and we should proceed to check the next orbit crossing T hours later.

286. If h is the simulation time within the current day that the satellite is known to be crossing latitude L ascending, and $\Delta h = h - H_A$, then the x-coordinates of the four points defining the coverage parallelogram will have their values shifted by adding the distance: $F_{TD}(-\Delta h)$.

Dealing With the Descending Half of the Orbit

287. The mathematics flips over identically when dealing with the descending half of the satellite's orbit. The satellite is moving from north to south now. The earth continues to rotate from west to east underneath it, of course. The net result is that the ascending parallelogram simply gets reflected. Taking the negative of all four x-coordinates in (J7)

gives the default parallelogram applicable to the descending portion. It is then positioned along the *x*-axis (east-west) using the identical arguments above based on the time it crosses the central latitude compared to the descending time, H_D.

288. The only additional detailed calculation required is the delay between the time the satellite ground track crosses the central latitude L ascending and the time it crosses L again descending. This fraction F is derivable from basic principles:

$$F = \frac{1}{2\pi}\cos^{-1}\left(2\sin^2 L\left(1+\frac{1}{\tan^2 I}\right)-1\right)$$
$$\Delta T = F \cdot T \qquad \text{(J9)}$$

289. Multiplying F with the orbital period T gives the time interval, ΔT, between ascending and subsequent descending crosses of latitude L (assumes L is north of the equator).

Summarizing the Satellite SD Generator Algorithm

290. In setup, the following parameters must be specified for the satellite SD Generator: the orbital inclination (I), the orbital period (T), the swath width of the sensor (S), and the ascending local time (H_A). Angles are in degrees, time in hours, and distance in nautical miles. The descending local time is calculated as $H_D = H_A \pm 12$ hours, whichever value is positive and not greater than 24.

291. Also given will be the parameters of the Regional View, specifically the central latitude (L), and the parameters X_{Max} and Y_{Max} that define the limits of the rectangular RV.

292. The time, t_0, of the first ascending crossing of latitude L can be specified in one of two ways. It is either specified directly by the user (so constellations of satellites can be coordinated), or is a random starting time drawn uniformly from the interval [0,T]. The time of the first descending crossing will be t_0*, which is either $t_0 + \Delta T$ or $t_0 + \Delta T - T$, whichever is positive and not greater than T, using ΔT as calculated in (J9).

293. Determine the first instance where the satellite will cross within the *ascending* window. Take the times $t = t_0$, $t_0 + T$, $t_0 + 2T$, …, $t_0 + nT$, … and determine the lowest value of n for which the residual day time - t minus (24 times the integer portion of t/24) - lies in the interval $H_A \pm \Delta H$, where ΔH has been determined via (J8).

294. Next, determine the first instance where the satellite will cross within the *descending* window. Take the times $t = t_0^*$, $t_0^* + T$, $t_0^* + 2T$, …, $t_0^* + mT$, … and determine the lowest value of m for which the residual day time - t minus (24 times the integer portion of t/24) - lies in the interval $H_D \pm \Delta H$.

295. Determine which mode, ascending or descending, will occur first and schedule a corresponding SD Generator event for that time in the future plus the applicable information latency time.

296. Upon completion of every satellite SD Generator event (SAT Event), the event's next occurrence will be scheduled. If the event represented an ascending pass, then

subtract off the latency time from the current time to give the actual time at which the satellite crossed *L*. Call this time t_1. The next descending crossing time will be $t_1^* = t_1 + \Delta T$. If the event represented a descending pass, then subtract off the latency time used from the current time to give the actual crossing time, t_1^*. The next ascending crossing time will be $t_1 = t_1^* + T - \Delta T$. Now plug these values into the process above, substituting t_1 and t_1^* for t_0 and t_0^* respectively. Then schedule the appropriate (ascending or descending) type of SD Generator event for the time calculated plus the assumed information latency time.

Annex K
Modelling Direction Finding Systems

297. An emitter on the Cartesian plane is being picked up by n stations, where $n > 1$. Each station can fix its bearing to the emitter. The error in this measurement is assumed to be Normally distributed with an angular standard deviation, σ, in degrees, that is the same for all stations.

298. The modelling approach is as follows. We will randomize a bearing from each station to the target about the known true bearing, and then find the pair of stations that has the least combined error in fixing the emitter's location. This process will define a region has the probability P (the global Positional Confidence Level) of including the actual SS target. This region is approximately parallelogram shaped, and is converted to a circle of equal area. Figure K-1 illustrates the constructs employed in this annex.

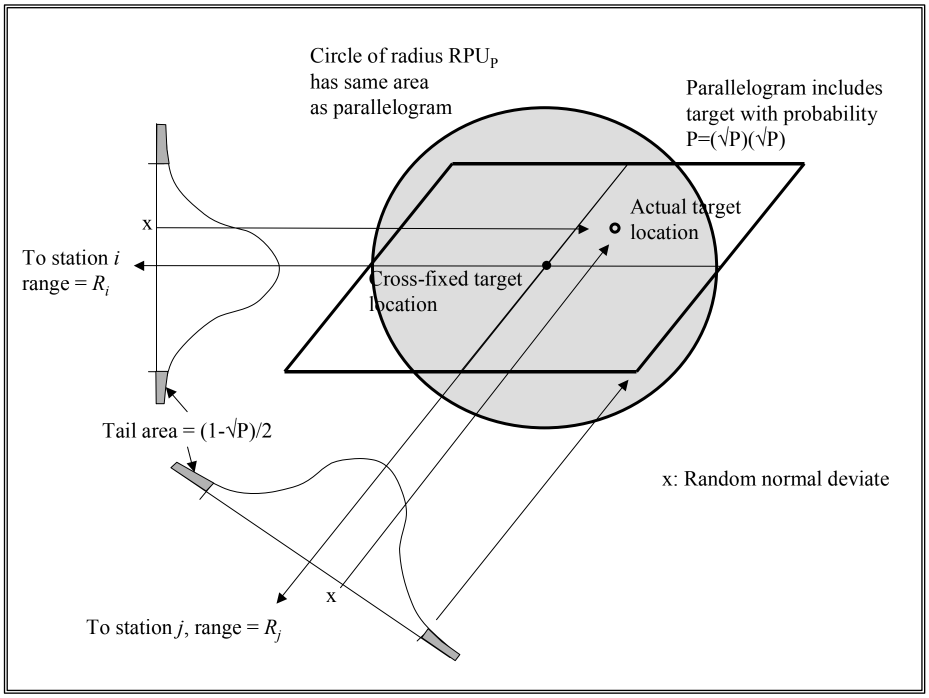

Figure K-1. *DF Event Modelling Constructs*

299. Given the coordinates of the target, (x_t,y_t), and the coordinates of each station, (x_i,y_i), the distance, D_i, and bearing, B_i, to the target from each station can be calculated.

$$D_i = \sqrt{(x_t - x_i)^2 + (y_t - y_i)^2}$$
$$B_i = \tan^{-1}\left(\frac{y_t - y_i}{x_t - x_i}\right) \qquad \text{(K1)}$$

300. Each station will make an estimate of B_i, call it b_i, which is based on a random standardized Normal deviate, r_i (see Annex B).

$$b_i = B_i + r_i\sigma \tag{K2}$$

301. Each pair of stations i and j will combine their bearing information to generate a cross-fixed position (x_{ij},y_{ij}), which is easily determined as a solution of two equations with two unknowns. The intersection position is

$$\begin{aligned} y_{ij} &= y_{ji} = \frac{m_j(x_i - x_j) + y_j - y_i(m_j / m_i)}{1 - m_j / m_i} \\ x_{ij} &= x_{ji} = \frac{y_{ij} - y_i + m_i x_i}{m_i} \\ where \quad & m_i = \tan b_i \;\; and \;\; m_j = \tan b_j \end{aligned} \tag{K3}$$

302. If slopes $m_i = m_j$ then the lines are parallel and there is no solution. If $m_i = 0$ then simply reverse the i and j above to calculate the solution.

303. Define d_{ij} and d_{jj} to be the distance from stations i and j, respectively, to the estimated target position cross-fixed using bearings from both

$$\begin{aligned} d_{ij} &= \sqrt{(x_{ij} - x_i)^2 + (y_{ij} - y_i)^2} \\ d_{ji} &= \sqrt{(x_{ij} - x_j)^2 + (y_{ij} - y_j)^2} \end{aligned} \tag{K4}$$

304. We will define the multiplicative factor f_p such that the angular interval, [b_i-$f_p\sigma$, b_i+$f_p\sigma$] has probability p of including the actual bearing to the target, B_i. The factor f_p is determined from the cumulative standardized Normal distribution. For example, if p = 0.95 then $f_{0.95}$ = 1.96. We will describe a method for calculating the inverse of the cumulative Normal shortly.

305. The angle $2f_p\sigma$, centred on b_i, projects a wider and wider swath as distance from the station increases. The width of the swath at the target is $2f_p\sigma(\pi/180)D_i$., where the $\pi/180$ factor performs the necessary conversion of degrees to radians.

306. For any two stations i and j fixing on the emitter, the two corresponding swaths intersect to create a four-sided shape. If we assume that the distances to the target are relatively large compared to the swath angle, then this shape is well approximated by a parallelogram centred on the estimated target location, as illustrated in Figure K-1.

307. This parallelogram has a probability p of including the target from station i, and the same probability from j, both assumed to be independent measurements. Therefore, the probability that the target is inside the intersection of the two swaths is the product of the two, or p^2. Since the objective is to ensure we localize the target to the level specified by the global Positional Confidence Level, P, we should use $p = \sqrt{P}$. We wish, therefore, to calculate $f_{\sqrt{P}}$.

308. Equation 26.1.23 on page 933 of Abramowitz and Stegun [11] provides a practical means of computing the inverse cumulative Normal function. The area in the upper tail of the standardized Normal distribution, $Q(z)$, is approximated by the following polynomial

$$Q(z) = \frac{1}{\sqrt{2\pi}} \int_z^\infty e^{-t^2/2} dt$$

$$\text{If } Q(z_q) = q, \text{ where } 0 < q \le 0.5, \text{ then}$$

$$z_q = t - \frac{c_0 + c_1 t + c_2 t^2}{1 + d_1 t + d_2 t^2 + d_3 t^3} \qquad \text{(K5)}$$

$$\text{where } t = \sqrt{\ln\left(\frac{1}{q^2}\right)} \text{ and}$$

$$c_0 = 2.515517, c_1 = .802853, c_2 = .010328,$$
$$d_1 = 1.432788, d_2 = .189269, d_3 = .001308$$

309. We wish to leave an area of $(1-\sqrt{P})/2$ in each tail of the Normal distribution. Therefore,

$$f_{\sqrt{P}} = z_q, \quad \text{where}$$
$$q = \frac{1-\sqrt{P}}{2} \qquad \text{(K6)}$$

310. We will leave it to the reader to show that the area of this parallelogram, L_{ij}, is:

$$L_{ij} = \frac{(2 f_{\sqrt{P}} (\sigma \pi / 180) d_{ij})(2 f_{\sqrt{P}} (\sigma \pi / 180) d_{ji})}{\left|\sin(b_i - b_j)\right|} \qquad \text{(K7)}$$

311. The algorithm selects the 'best' pair of stations, taken as that pair of stations with the smallest area for localizing the actual position of the target. Hence, we select the pair of stations that yields the lowest value of L_{ij}.

312. Finally, we convert the parallelogram to a circle of the same area. The radius of positional uncertainty at the P probability level, RPU_P, can then be calculated. The final output is:

$$\text{Select stations } k, l \text{ such that} \quad L_{kl} = \underset{i,j}{Min}\left(L_{ij}\right)$$
$$\text{Estimated tgt position : } \quad (x_{kl}, y_{kl})$$
$$RPU_P = \sqrt{L_{kl} / \pi}$$

This page intentionally left blank.

Annex L
Assigning a Velocity Vector to a Tracked Target

313. When a Sensor Datum is matched to a Tracked Target, there are three possible velocity vectors that can be assigned.

a. The SD velocity vector determined by the sensor. The associated speed and heading error parameters are those of the sensor.

b. The old velocity vector for the TT determined at the time of the last update for that TT.

c. The calculated velocity vector based on time differencing between the estimated position at the previous update and the current estimated position. The associated speed and heading error parameters are the global parameters assigned to all estimates based on time differencing.

314. The last vector is easily calculated, but the procedure to calculate it is outlined below for the sake of completeness. Let (x_o,y_o) be the old estimated position of the TT at the previous update time. Let (x_c,y_c) be the new estimated position, which is the centre of the region of intersection of the two circles, as calculated by equation (E14). Note that (x_o,y_o) is *not* necessarily the centre of the TT circle that is being intersected, as these circles are estimates of position at the *current* time (they account for the possible blending of dead-reckoning based on the Heading Consistency Factor). Let Δt be the difference between the current time and the last update time for the TT. The new speed, S, and heading, H, are:

$$
\begin{aligned}
&v_x = (x_c - x_o)/\Delta t \\
&v_y = (y_c - y_o)/\Delta t \\
&S = \sqrt{v_x^2 + v_y^2} \\
&H = \tan^{-1}\left(\frac{x_c - x_o}{y_c - y_o}\right)\cdot\frac{180}{\pi} \\
&\text{if } (y_c - y_o) < 0 \text{ add } 180^\circ \text{ to } H \\
&\text{if } (y_c - y_o) = 0 \text{ and } (x_c - x_o) \geq 0 \text{ then } H = 90^\circ \\
&\text{if } (y_c - y_o) = 0 \text{ and } (x_c - x_o) < 0 \text{ then } H = 270^\circ
\end{aligned}
\qquad \text{(L1)}
$$

315. Since the SS's real velocity vector could change at any time, it makes sense to select the most current estimate. This is at least an arguable statement as there may be large differences in accuracy between the estimates. Am I better off selecting a very accurate velocity vector estimate from a previous update 6 hours ago, or a much less accurate but current estimate? Or should I select an accurate sensor input that has a large latency, making it staler than the less accurate value assigned at the last update. It is difficult to convince oneself that the staler estimate, even if it is more accurate, is superior.

316. Therefore, the following velocity vector assignment heuristic will be employed.

Condition A: Sensor latency exceeds time since last update.

317. In this situation, the SD value is staler than the TT value set at the previous update. Since the differencing calculation vector c. is also calculated using the staler position and velocity vector information from the SD, vector b. will be retained as the velocity vector for the updated TT.

Condition B: Sensor latency is less than time since last update.

318. Now the sensor value is more current than the velocity vector from the previous update. Vector b. is rejected as being too stale.

319. So we will choose between the vectors a. and c. above (assuming the sensor generated a velocity vector estimate). The measure used to compare them is the product of the following three parameters: the estimated target speed; the standard deviation of the speed estimate; and the standard deviation of the heading estimate. As shown in the discussion that preceded equation (D4) in Annex D, this product is proportional to the dead-reckoning position estimation error. Select the velocity vector estimate, a. or c. above, which produces the smallest product.

Distribution List

3353-1 (DRDC CORA/DOR(MLA))

April 2006

DISTRIBUTION OF DRDC CORA TECHNICAL REPORT TR 2006/05 "DESIGN SPECIFICATIONS: SIMULATION OF SURFACE SURVEILLANCE SYSTEM-OF-SYSTEMS SUCCESS ('S6')"

1. This report documents the design specifications for the 'S6' model, an Operational Research tool that will support coastal surveillance effectiveness studies. No single surface surveillance asset has the presence, scope, and fidelity to perform this surveillance function completely by itself. The ideal solution will be a 'system of systems' that relies on different surveillance systems with diverse spatial, temporal, and information content characteristics working together to deliver a clear Recognized Maritime Picture (RMP).

2. The S6 model will enable combinations of different sensors and platforms to be evaluated. It will be a Monte Carlo simulation of surface ship traffic, the performance of various surveillance assets operating on that traffic, and the integration of the sensor information into a RMP over time. This model will be developed under contract to the specifications outlined in this document, and will be jointly funded by the DRDC Centre for Operational Research & Analysis (CORA) and the Chief of the Air Staff (CAS).

3. Questions or comments are welcome and can be directed to the author, Mr. D. Mason, at 992-8507.

M.T. Rey
Director General, Centre for Operational Research & Analysis

Enclosure: 1

Distribution List

External

CFAWC
CFMWC
DRDC Atlantic
DRDC Ottawa
MARLANT N02OR
MARPAC N02OR
1 Cdn Air Div HQ/ORAD

NORAD HQ, Attn: V. Fong

Internal

DGSP
DGJFD
CANADA COM
DG Air FD
D Air SP
D Mar Strat
DLSP
DDA
CORA Chief Scientist
DOR(MLA)
DOR(Joint)
DASOR
MORT
LFORT
SPORT
JSORT
CORT
DRDC/DRDKIM3 (PDF file)
CORA Library (1 copy plus PDF file)
Author (6)

DOCUMENT CONTROL DATA
(Security classification of title, body of abstract and indexing annotation must be entered when the overall document is classified)

1. ORIGINATOR (the name and address of the organization preparing the document. Organizations for whom the document was prepared e.g. Establishment Sponsoring a contractor's report, or tasking agency, are entered in Section 8).

DRDC – Centre for Operational Research and Analysis
101 Colonel By Drive, Ottawa, ON K1A 0K2

2. SECURITY CLASSIFICATION (overall security classification of the document, including special warning terms if applicable)

UNCLASSIFIED

3. TITLE (the complete document title as indicated on the title page. Its classification should be indicated by the appropriate abbreviation (S, C or U) in parentheses after the title)

Design Specifications: Simulation of Surface Surveillance System-of-Systems Success ('S6')

4. AUTHORS (last name, first name, middle initial)

Mason, D.W.

5. DATE OF PUBLICATION (month Year of Publication of document)

April 2006

6a. NO OF PAGES (total containing information. Include Annexes, Appendices, etc.)

88

6b. NO OF REFS (total cited in document)

12

7. DESCRIPTIVE NOTES (the category of document, e.g. technical report, technical note or memorandum. If appropriate, enter the type of report e.g. interim, progress, summary, annual or final. Give the inclusive dates when a specific reporting period is covered.)

DRDC CORA Technical Report

8. SPONSORING ACTIVITY (the name of the department project office or laboratory sponsoring the research and development. Include the address).

N/A

9a. PROJECT OR GRANT NO. (if appropriate, the applicable research and development project or grant number under which the document was written. Please specify whether project or grant.)

N/A

9b. CONTRACT NO. (if appropriate, the applicable number under which the document was written.)

N/A

10a. ORIGINATOR's document number (the official document number by which the document is identified by the originating activity. This number must be unique to this document.)

DRDC CORA TR 2006-05

10b. OTHER DOCUMENT NOS. (Any other numbers which may be assigned this document either by the originator or by the sponsor.)

11. DOCUMENT AVAILABILITY (any limitations on further dissemination of the document, other than those imposed by security classification.)

(X) Unlimited distribution
( ) Distribution limited to defence departments and defence contractors: further distribution only as approved
( ) Distribution limited to defence departments and Canadian defence contractors; further distribution only as approved
( ) Distribution limited to government departments and agencies; further distribution only as approved
( ) Distribution limited to defence departments; further distribution only as approved
( ) Other (please specify):

12. DOCUMENT ANNOUNCEMENT (any limitation to the bibliographic announcement of this document. This will normally correspond to the Document Availability (11). However, where further distribution (beyond the audience specified in 11) is possible, a wider announcement audience may be selected.)

13. ABSTRACT (a brief and factual summary of the document. It may also appear elsewhere in the body of the document itself. It is highly desirable that the abstract of classified documents be unclassified. Each paragraph of the abstract shall begin with an indication of the security classification of the information in the paragraph (unless the document itself is unclassified) represented as (S), (C), or (U). It is not necessary to include here abstracts in both official languages unless the test is bilingual).

In today's world of global terrorism it is more critical than ever for Canada to have full knowledge of the nature of surface traffic off Canada's coastlines. No single surface surveillance asset has the presence, scope, and fidelity to perform this function completely by itself. The ideal solution will be a 'system of systems' that relies on different surveillance systems with diverse spatial, temporal, and information content characteristics working together to deliver a clear Recognized Maritime Picture (RMP). Examples of specific systems that might contribute are aircraft patrols, ship patrols, unmanned aerial vehicles, radio direction finding systems, surveillance satellites, ground-based radars, surface wave radars, or automatic identification systems (AIS).

Determination of the ideal system-of-systems requires an analytical capability to assess the effectiveness of specific combinations of systems. The preferred method for satisfying this requirement is through the development of a simulation of surface traffic, the performance of various surveillance assets operating on that traffic, and the integration of the sensor information into a RMP over time. This will be realized as the Simulation of Surface Surveillance System-of-Systems Success, or the 'S6' model, which will be developed under contract to the specifications outlined in this document.

The S6 Model will be an event-based simulation of surface ship traffic and sensor activity over an area of operations, typically one of Canada's ocean approaches. Rogue vessel tracks will be injected into the background surface traffic and the simulation will be able to assess how well the combined system-of-systems responded in acquiring these rogue vessels. There are Monte-Carlo aspects to the simulation, specifically in the generation of ship traffic and errors introduced by each sensor system in acquiring targets.

14. KEYWORDS, DESCRIPTORS or IDENTIFIERS (technically meaningful terms or short phrases that characterize a document and could be helpful in cataloguing the document. They should be selected so that no security classification is required. Identifiers, such as equipment model designation, trade name, military project code name, geographic location may also be included. If possible keywords should be selected from a published thesaurus, e.g. Thesaurus of Engineering and Scientific Terms (TEST) and that thesaurus-identified . If it is not possible to select indexing terms which are Unclassified, the classification of each should be indicated as with the title.)

Simulation
Surveillance
Intelligence, Surveillance, and Reconnaissance (ISR)
Surface Ships
Event based simulation
Monte Carlo
Data Fusion
Circular Normal Distribution
Rayleigh Distribution
Air Patrol
Surface Wave Radar
Satellite surveillance
High Frequency Direction Finding
Automatic Identification System
Operational Research
Modelling